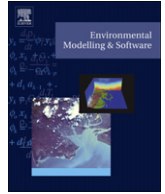


Contents lists available at [SciVerse ScienceDirect](http://SciVerse.Sciencedirect.com)

Environmental Modelling & Software

journal homepage: www.elsevier.com/locate/envsoft

Model of the Regional Coupled Earth system (MORCE): Application to process and climate studies in vulnerable regions

Philippe Drobinski^{a,*}, Alesandro Anav^a, Cindy Lebeau-pin Brossier^{a,b}, Guillaume Samson^c, Marc Stéfanon^a, Sophie Bastin^d, Mélika Baklouti^e, Karine Béranger^b, Jonathan Beuvier^{b,f,g}, Romain Bourdallé-Badie^{f,h}, Laure Coquart^h, Fabio D'Andrea^a, Nathalie de Noblet-Ducoudréⁱ, Frédéric Diaz^e, Jean-Claude Dutayⁱ, Christian Ethé^j, Marie-Alice Foujols^j, Dmitry Khvorostyanov^a, Gurvan Madec^c, Martial Mancip^j, Sébastien Masson^c, Laurent Menut^a, Julien Palmieriⁱ, Jan Polcher^a, Solène Turquet^a, Sophie Valcke^h, Nicolas Viovyⁱ

^aLaboratoire de Météorologie Dynamique, Institut Pierre Simon Laplace, CNRS/Ecole Polytechnique/UPMC/ENS, Palaiseau, France

^bEcole Nationale Supérieure de Techniques Avancées-ParisTech, Palaiseau, France

^cLaboratoire d'Océanographie et du Climat – Expérimentation et Approches Numériques, Institut Pierre Simon Laplace, CNRS/UPMC/IRD/MNHN, Paris, France

^dLaboratoire Atmosphères, Milieux, Observations Spatiales, Institut Pierre Simon Laplace, CNRS/UVSQ/UPMC, Paris, France

^eMediterranean Institute of Oceanography, CNRS/Aix-Marseille Université/IRD/Université du Sud Toulon-Var, Marseille, France

^fMercator Ocean, Toulouse, France

^gCentre National de Recherches Météorologiques, Météo-France/CNRS, Toulouse, France

^hCentre Européen de Recherche et de Formation Avancée en Calcul Scientifique, Toulouse, France

ⁱLaboratoire des Sciences du Climat et de l'Environnement, Institut Pierre Simon Laplace, CNRS/CEA/UVSQ, Gif sur Yvette, France

^jInstitut Pierre Simon Laplace, CNRS, Paris, France

ARTICLE INFO

Article history:

Received 22 June 2011

Received in revised form

18 January 2012

Accepted 30 January 2012

Available online xxx

Keywords:

MORCE platform
Regional Earth system
Climate modeling
Mesoscale process
Impact studies
HyMeX
ChArMeX
MerMeX
CORDEX

ABSTRACT

The vulnerability of human populations and natural systems and their ability to adapt to extreme events and climate change vary with geographic regions and populations. Regional climate models (RCM), composed by an atmospheric component coupled to a land surface scheme and driven over ocean areas by prescribed sea surface temperature, have been developed to produce fine scale regional climate change information useful for impact assessment and adaptation studies. Although RCM can be sufficient for many applications, the Earth system is composed of the physical, chemical, biological, and social components, processes, and interactions that together determine the state and dynamics of Earth, including its biota and human occupants. Developing regional Earth system models has thus two primary motivations: (1) with respect to climate science, to improve modeling capabilities and better understand coupled processes at regional scales and (2) to support stakeholders who aim to use climate information for regionally-specific impact assessment and adaptation planning. IPSL in collaboration with ENSTA-ParisTech, LOPB, and CERFACS developed the MORCE (Model of the Regional Coupled Earth system) platform for process and climate studies of the regional Earth system. The original aspects of the MORCE platform are (1) the integration of a large number of coupled compartments and processes (physical and biogeochemical processes in the ocean, atmosphere and continent), (2) the transferability of the numerical platform to different locations in the world, (3) the use of a non-hydrostatic model for the atmospheric module which allows an accurate representation of kilometeric scale processes. The present article describes the MORCE platform, detailing its various modules and their coupling and illustrating its potential with results obtained in the Mediterranean region and over the Indian Ocean.

© 2012 Elsevier Ltd. All rights reserved.

1. Introduction

The Fourth IPCC Assessment Report forecasts an increase in the Earth's average temperature ranged between 1.4 °C and 5.8 °C over the 21st century, accompanied by a rise in sea levels between 9 and 88 cm (IPCC, 2007). This rapid change in the global climate may

* Corresponding author.

E-mail address: philippe.drobinski@lmd.polytechnique.fr (P. Drobinski).

result in the modification of the frequency and intensity of extreme events and natural disasters (cyclones, droughts, floods, etc...) in certain parts of the world. Among other consequences, these changes are set to cause radical disruption to agriculture, large population movements as people abandon disaster-struck regions (such as flooded coastal plains and areas blighted by desertification) for less-affected areas, and heightened political tensions.

The vulnerability of human populations and natural systems in the face of climate change varies greatly according to geographic regions and populations. The natural and social systems in each region vary, resulting in differences in the ability to adapt to the impact of current and future climate changes. Furthermore, each regional system is affected both by large-scale climate teleconnections and by specific local processes. As these differences raise a number of serious concerns, it appears crucial to fully understand the space–time interactions that occur at the regional scale, with particular focus on past variability and vulnerability of key regions to a range of constraints.

A number of regional climate model (RCM) systems have been developed during the last two decades in order to downscale the outputs from large-scale global climate model (GCM) simulations and produce fine scale regional climate change information useful for impact assessment and adaptation studies (e.g. Giorgi, 2006a). To date, most RCMs have been mainly composed of an atmospheric component coupled with a land surface scheme. Indeed, the land surface plays a pivotal role in the Earth system through physical, biophysical and biogeochemical interaction with the atmosphere and oceans (Foley et al., 1994; Prentice et al., 2000). Land-atmosphere interactions include complex feedbacks between soil, vegetation, and atmosphere through the exchanges of water, momentum, energy, and greenhouse gases (Pielke et al., 1998; Arora, 2002), as well as the emission/deposition of several compounds (e.g. Guenther et al., 2006; Lathiere et al., 2006; Petroff et al., 2008). RCMs have also been driven over ocean areas by prescribed sea surface temperature.

Although such a RCM can be sufficient for many applications, there are cases in which the fine scale feedbacks associated with air–sea interactions can substantially influence the spatial and temporal structure of regional climates. A typical example is the Indian Ocean and its effects on the South Asia monsoon, for which it has been clearly shown that air–sea feedbacks are essential in regulating the development of the South Asia monsoon (e.g. Meehl, 1994). Ratnam et al. (2008) coupled the regional atmospheric model RegCM3 (Pal et al., 2007) with the regional ocean model POM (Mellor, 2004) over the Indian ocean and found that the coupling considerably improved the simulation of the Indian monsoon rain band over both the ocean and land areas. The Max-Planck atmosphere–ocean regional climate model (AORCM) has been employed over the Indonesian region (Aldrian et al., 2005), with a remarkable improvement in the simulation of rainfall. Different AORCMs have also been developed for the Baltic Sea region (Döscher et al., 2002; Lehmann et al., 2004) and for the Arctic region (Rinke et al., 2003). Strong air–sea interactions take place as well in the Mediterranean basin, one of the most vulnerable to global warming (Giorgi, 2006b). The morphological complexity of the basin leads to the formation of intense weather phenomena, such as topographically-induced strong winds (e.g. Drobinski et al., 2001, 2005; Guénard et al., 2005, 2006; Salameh et al., 2010), intense cyclogenesis (e.g. Alpert et al., 1995), heavy precipitation (e.g. Ducrocq et al., 2008). Such physical processes have two critical characteristics: first, they derive from strong air–sea coupling and, second, they occur at fine spatial scales (e.g. Lebeaupin et al., 2006; Lebeaupin Brossier et al., 2009; Lebeaupin Brossier and Drobinski, 2009). In order to explicitly resolve the two-way interactions at the atmosphere–ocean interface in the Mediterranean region, Somot et al. (2008) coupled the global

atmospheric model ARPEGE with the regional ocean model OPAMED (Somot et al., 2006). A similar development was conducted by Artale et al. (2009) with the PROTHEUS system integrating RegCM3 and the MITgcm (Marshall et al., 1997a,b) models as the atmospheric and oceanic component, respectively. Comparison of coupled and uncoupled experiments showed that in the coupled simulations the climate change signal was generally more intense over large areas, with wetter winters over northern Europe and drier summers over southern and eastern Europe. The better simulated Mediterranean SST appeared to be one of the factors responsible for such differences, which were found to be highly significant.

However, the Earth system is the physical, chemical, biological, and social components, processes, and interactions that together determine the state and dynamics of Earth, including its biota and human occupants. Developing regional Earth system models has two primary motivations: (i) with respect to climate science, to improve modelling capabilities and better understand coupled processes at regional scales and (ii) to support stakeholders who aim to use climate information for regionally-specific impact assessment and adaptation planning. There is thus a need to develop what amounts to an enhanced Earth system simulator to improve our ability to anticipate impacts of a given set of human actions or conditions on global and regional climate and on biological, geochemical, and hydrological systems on seasonal to decadal time scales. Most current efforts to build state-of-the-art whole-Earth system models consist in complementing sophisticated geophysical kernels (AORCMs based on exact dynamical equations like Navier–Stokes) by tools representing other parts of the planetary makeup, as for example marine-biosphere or atmospheric chemistry models. This is particularly true for the global Earth system simulator, but not fully achieved at regional scale, while this is needed to assess the potential impact of environmental changes on regional economic conditions, food security, water supplies, health, biodiversity, and energy security, in particular in poor and vulnerable communities.

The Institut Pierre Simon Laplace (IPSL) in collaboration with Ecole Nationale Supérieure de Techniques Avancées-ParisTech (ENSTA-ParisTech), Laboratoire d'Océanographie Physique et Biogéochimique (LOPB) and Centre Européen de Recherche et de Formation Avancée en Calcul Scientifique (CERFACS), developed the MORCE (Model of the Regional Coupled Earth system) platform for process and climate studies of the Regional Earth system. The original aspects of the MORCE platform are:

1. the integration of a large number of coupled compartments and processes (physical and biogeochemical processes in the ocean, atmosphere and continent),
2. the transferability of the numerical platform to different locations in the world,
3. the use of a non-hydrostatic model for the atmospheric module which allows the representation of kilometric scale processes for which the non-hydrostatic assumption does not stand.
4. the two-way grid nesting capability of both the atmospheric and oceanic components which allows very high resolution of the coupled system in a model subdomain.

This platform has been applied over two different vulnerable regions, i.e. the Mediterranean basin and the Indian Ocean (Fig. 1). Configurations are under development for the entire Tropical band. The MORCE platform is at present used to investigate the coupling between various processes in these regions but also for dynamical downscaling in the Mediterranean region in the framework of the Hydrological cycle in the Mediterranean experiment (HyMeX) (Drobinski et al., 2009a,b, 2010) and the Coordinated Downscaling

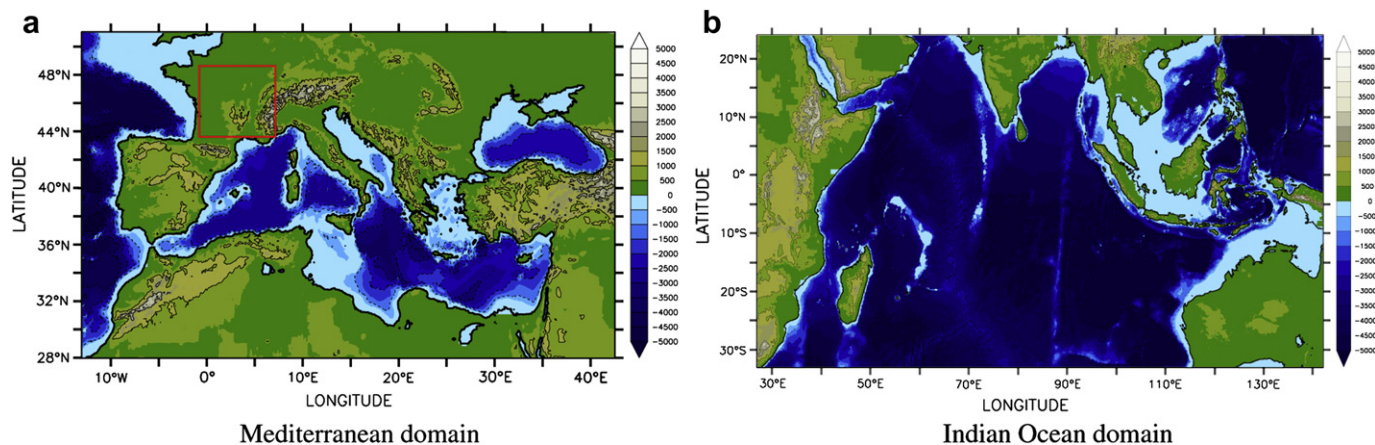


Fig. 1. Examples of existing MORCE platform domains. The color code indicates the height of the topography and the depth of the bathymetry. The red box in panel a is a zoom on the domain used to illustrate the impact of vegetation/water cycle feedback on the 2003 summer heat wave in sub-section 5.1. (For interpretation of the references to colour in this figure legend, the reader is referred to the web version of this article.)

Experiment (CORDEX) of the World Climate Research Program (WCRP) (Giorgi et al., 2009). In the near-future, it should be used in the frame of the Chemistry-Aerosol Mediterranean Experiment (ChArMeX; Dulac, 2011) and the Marine Ecosystems' Response in the Mediterranean Experiment (MerMeX; The MerMex Group, 2011) of the Mediterranean Integrated STudies at Regional And Local Scales (MISTRALS) international program.

After the introduction in Section 1, Section 2 describes the different modules of the MORCE platform. Section 3 describes the different types of coupling techniques and the nature of the data exchanged between the different modules. Section 4 details the management of the MORCE platform. Section 5 illustrates with scientific results the application of the MORCE platform over the Mediterranean basin and the Indian Ocean. Finally, Section 6 concludes the description of version 1 of the MORCE platform and gives some short-term perspectives of evolution and development towards version 2 of the MORCE platform.

2. MORCE modules

The MORCE modeling platform is divided into 5 modules:

1. the atmospheric module (ATM)
2. the oceanic module (OCE)
3. the hydrological and vegetation module (LSM)
4. the atmospheric chemistry module (CHEM)
5. the marine biogeochemistry module (BIOGEOCHEM)

2.1. ATM module

The atmospheric module is based on the dynamical core of the numerical model WRF (Weather Research and Forecasting). The WRF model is developed by the National Center for Atmospheric Research (NCAR) (Skamarock et al., 2008). The model solves the non-hydrostatic equations of motion in terrain following sigma coordinates. A complete set of physics parametrizations is available and several sensitivity studies have been performed to quantify uncertainties in regional climate modeling (e.g. Flaounas et al., 2010; Cretat et al., 2011).

The motivation for the use of a non-hydrostatic atmospheric model is twofold:

- for process studies requiring the simulation of very fine scale processes (generally few days simulations), the hydrostatic

assumption is not verified anymore. For instance explicit convection, mountain wave breaking, mountain wakes are non-hydrostatic weather phenomena which thus need an adapted physics.

- regarding regional climate applications, the trend is towards the increase of the horizontal resolution to explicitly simulate fine-scale processes in order to quantify their contribution to the regional climate. At present, typical resolution of few tens of kilometers do not require a non-hydrostatic model but with increasing computer efficiency, horizontal resolution of few kilometers for such applications will soon be possible.

The grid nesting capacity is a strong added value of WRF which allows to refine the simulation from a resolution of few tens of kilometers over a large domain, for which hydrostatic assumption holds, down to kilometer-scale resolution over regions of interest for which non-hydrostatic capacity is mandatory (see WRF documentation reference in Table A.2 in the appendix). In the context of the MORCE platform, such grid nesting capacity can be used since the OCE module NEMO also has similar grid nesting capacity (see below).

2.2. OCE module

The ocean model is the NEMO system of IPSL (Madec, 2008) in regional configurations over the standard horizontal grid ORCA. Vertical stretched z-levels are used, except for the bottom layer for which a partial-cell parameterization is used, allowing the last free level of the model to fit the bathymetry. The filtered free surface of Roulet and Madec (2000) is used. The solar heat flux can penetrate the ocean surface layer (Bozec et al., 2008). As discussed above, a key added value of NEMO is also its grid nesting capacity (see NEMO documentation reference in Table A.2 in the appendix) which allows grid refinement to kilometer-scale resolution which is fully compatible with the ATM module WRF. The ocean grid resting capability is provided through the use of the Adaptive Grid Refinement In Fortran (AGRIF) package (Debreu et al., 2008).

At present, two configurations of the MORCE platform are operational for the Mediterranean Sea and the Indian Ocean (Fig. 1). Two configurations are under development for West Africa and the Gulf of Guinea in the Tropical Atlantic Ocean, and for South America and Eastern Tropical Pacific Ocean. The specificities of each ocean regional configuration mainly lie on the boundary condition formulation (see details in Section 5).

2.3. LSM module

The ATM module (WRF) already includes “classical” interactive land-surface models that compute the heat and moisture flux from soil water content and temperature. However, these land-surface models (LSM) have a low degree of sophistication and do not include carbon cycle and dynamic vegetation. In addition to these LSMs, the MORCE platform includes the land-surface model ORCHIDEE (ORganizing Carbon and Hydrology In Dynamic Ecosystems) developed at IPSL and Laboratoire de Glaciologie et Géophysique de l'Environnement (LGGE). It is an LSM coupled to a biogeochemistry and a dynamic biogeography model (Krinner et al., 2005). ORCHIDEE simulates the fast feedback occurring between the vegetated land surface and the atmosphere, the terrestrial carbon cycle, and also changes in vegetation composition and distribution in response to climate change.

ORCHIDEE is based on three different modules (Krinner et al., 2005). The first module, called SECHIBA (Ducoudré et al., 1993; de Rosnay and Polcher, 1998), describes the fast processes such as exchanges of energy and water between the atmosphere and the biosphere, and the soil water budget. Its time step is that of the driving ATM module ($\Delta t_{CPL} = \Delta t_{ATM}$, see Table 1 and Fig. 2). SECHIBA also includes a routing module which transports the water which is not infiltrated or drains at the bottom of the soil through rivers and aquifers (d'Orgeval et al., 2008). This module runs at the spatial resolution of ORCHIDEE but represents more than one basin per grid box. The time step is larger than the one of SECHIBA and depends on the horizontal resolution. The tight integration of the routing within SECHIBA allows to re-evaporate the water on its way to the ocean through processes such as floodplains or irrigation (de Rosnay et al., 2003). The phenology and carbon dynamics of the terrestrial biosphere are simulated by the STOMATE (Saclay Toulouse Orsay Model for the Analysis of Terrestrial Ecosystems) model (Krinner et al., 2005). STOMATE simulates, with a daily time step,

processes as photosynthesis, carbon allocation, litter decomposition, soil carbon dynamics, maintenance and growth respiration, and phenology. Finally, the long-term processes (yearly time step) include vegetation dynamics, fire, sapling establishment, light competition, and tree mortality are simulated according to the global vegetation model LPJ (Sitch et al., 2003).

In the ORCHIDEE model, the land surface is described as a mosaic of twelve plant functional types (PFTs) and bare soil. The definition of PFT is based on ecological parameters such as plant physiognomy (tree or grass), leaves (needleleaf or broadleaf), phenology (evergreen, summergreen or raingreen) and photosynthesis type for crops and grasses (C3 or C4). Relevant biophysical and biogeochemical parameters are prescribed for each PFT (Krinner et al., 2005). The PFT distribution can be either prescribed from an input inventory (static mode, LPJ deactivated), or entirely simulated by the model depending on climate conditions (dynamic mode, LPJ activated). The fraction of grid space covered by agricultural croplands is always prescribed, so that crop extent is not affected by dynamic vegetation change. Plant assimilation in ORCHIDEE model is based on Farquhar model (Farquhar et al., 1980) for C3 plants and Collatz et al. (1992) for C4 plants. Maintenance respiration is a function of each living biomass pool and temperature, while growth respiration is computed as a fraction of the difference between assimilation inputs and maintenance respiration outputs to plant biomass.

2.4. CHEM module

The pollutants concentrations are calculated by the CHIMERE chemistry-transport model (CTM) (Bessagnet et al., 2010). This model is developed by IPSL and Institut National de l'Environnement Industriel et des Risques (INERIS). This CTM is an off-line model and needs to be driven by an atmospheric dynamical model, i.e. WRF in the MORCE platform (ATM module). CHIMERE

Table 1
Meaning of variable names of Fig. 2 with the corresponding unit and data transfer. The data exchange time step Δt_{CPL} is indicated in the right column: Δt_{ATM} is the ATM integration time step, Δt_{OCE} is the OCE integration time step and $\Delta t_{ATM/OCE}$ is the ATM/OCE coupling time step. The ATM/OCE coupling time step $\Delta t_{ATM/OCE}$ is for example 1 h for the Indian Ocean configuration and 3 h for the Mediterranean configuration (see Section 5).

| Variable name | Variable | Unit | Variable transfer | Coupling interval Δt_{CPL} |
|---------------------------------|---|--------------------------------------|-------------------|------------------------------------|
| t2m | 2-m temperature | K | ATM → LSM | Δt_{ATM} |
| qsfc | Surface moisture | kg kg ⁻¹ | ATM → LSM | Δt_{ATM} |
| u1, v1 | First model level wind components | m s ⁻¹ | ATM → LSM | Δt_{ATM} |
| psfc | Surface pressure | hPa | ATM → LSM | Δt_{ATM} |
| SWN | Net surface short wave radiation | W m ⁻² | ATM → LSM | Δt_{ATM} |
| SWD | Downward surface short wave radiation | W m ⁻² | ATM → LSM | Δt_{ATM} |
| LWD | Downward surface long wave radiation | W m ⁻² | ATM → LSM | Δt_{ATM} |
| C _{drag} | Drag coefficient | – | ATM → LSM | Δt_{ATM} |
| P | Precipitation | mm | ATM → LSM | Δt_{ATM} |
| SH | Surface sensible heat flux | W m ⁻² | LSM → ATM | Δt_{ATM} |
| LH | Surface latent heat flux | W m ⁻² | LSM → ATM | Δt_{ATM} |
| α | Albedo | – | LSM → ATM | Δt_{ATM} |
| ε | Surface emissivity | W m ⁻² | LSM → ATM | Δt_{ATM} |
| TSK | Skin temperature | K | LSM → ATM | Δt_{ATM} |
| ET | Evapo-transpiration | mm | LSM → ATM | Δt_{ATM} |
| runoff | Runoff (river flow and coastal flow) | m ³ s ⁻¹ | LSM → ATM | Δt_{ATM} |
| LAI | Leaf Area Index | m ² m ⁻² | LSM → ATM | Δt_{ATM} |
| LAI | Leaf Area Index | m ² m ⁻² | LSM → CHEM | 1 day |
| C _p | Canopy conductance | cm s ⁻¹ | LSM → CHEM | 1 h |
| O ₃ | Ozone concentration | ppb | CHEM → LSM | 1 h |
| SWN | Net surface short wave radiation | W m ⁻² | ATM → OCE | $\Delta t_{ATM/OCE}$ |
| LWN–LH–SH | Non-solar heat flux (net long wave radiation – latent heat – sensible heat) | W m ⁻² | ATM → OCE | $\Delta t_{ATM/OCE}$ |
| E – P | Net fresh water = Evaporation – Precipitation | kg m ⁻² s ⁻¹ | ATM → OCE | $\Delta t_{ATM/OCE}$ |
| τ_x, τ_y | Wind stress components | N m ⁻² | ATM → OCE | $\Delta t_{ATM/OCE}$ |
| SST | Sea Surface Temperature | K | OCE → ATM | $\Delta t_{ATM/OCE}$ |
| T | Ocean temperature | K | OCE → BIOGEOCHEM | Δt_{OCE} |
| PAR | Downward Photosynthetically Active Radiation | W m ⁻² | OCE → BIOGEOCHEM | Δt_{OCE} |
| C _b | Biogeochemical concentrations | mmol m ⁻³ | OCE → BIOGEOCHEM | Δt_{OCE} |
| S _o – S _i | Sources less Sinks (tendencies) | mmol m ⁻³ s ⁻¹ | BIOGEOCHEM → OCE | Δt_{OCE} |

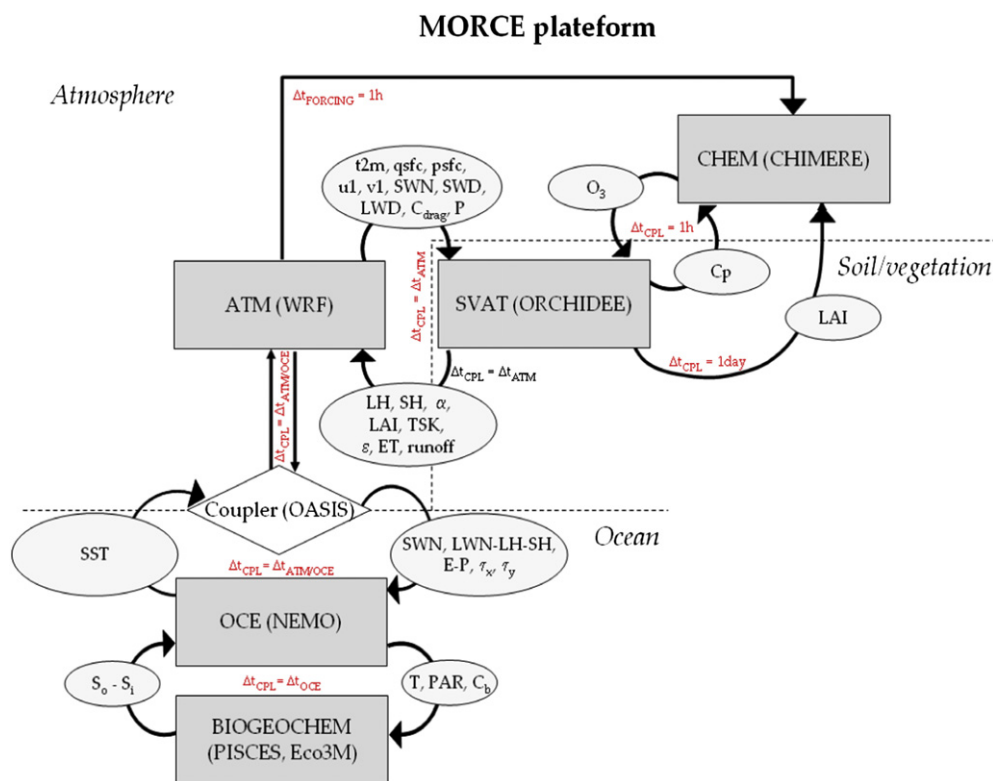


Fig. 2. MORCE platform version 1 flow chart.

has similar grid nesting capacity as the ATM module WRF. CHIMERE calculates, given a set of nitrogen oxide (NO_x), sulphur oxide (SO_x), ammonia (NH_3), particulate matter (PM), volatile organic compounds (VOCs) and carbon monoxide (CO) emissions, the concentrations of 44 gas-phase and aerosol species. It has been operated over many regions with horizontal grid-resolution from a few kilometers (Vautard et al., 2003; Valari and Menut, 2010) to one degree (Bessagnet et al., 2008; Menut and Bessagnet, 2010). The dynamics and gas-phase parts of the model are described in Schmidt et al. (2001), and improvements have successively been brought (Vautard et al., 2005; Bessagnet et al., 2008). For both ozone (O_3) and PM_{10} (particles of 10 μm or less), the model has undergone extensive modeled aerosols intercomparisons at European and city scales (Vautard et al., 2007; Van Loon et al., 2007; Schaap et al., 2007). The aerosols model species are sulfates, nitrates, ammonium, secondary organic aerosols, sea-salt (considered as inert here) and dust. The particle size distribution ranges from about 40 nm to 10 μm and are distributed into 8 bins (from 0.04 to 10 μm). The gas-particle partitioning of the ensemble Sulfate/Nitrate/Ammonium is treated by the code ISORROPIA (Nenes et al., 1998) implemented in CHIMERE. The surface emissions are constituted of anthropogenic and biogenic emissions. The anthropogenic emissions are taken from the Co-operative Programme for Monitoring and Evaluation of the Long-range Transmission of Air pollutants in Europe – EMEP – (Vestreng, 2003). Aerosol emissions feed the model species denoted as “primary particle material” (PPM), which contains several compounds (such as black and organic carbon) coming from various anthropogenic sources. The biogenic emissions are diagnosed using the MEGAN model (Guenther et al., 2006). MEGAN parameterizes the bulk effect of changing environmental conditions using three time-dependent input variables specified at the top of the canopy: temperature (T, K), radiation (PPFD, $\mu\text{mol m}^{-2} \text{s}^{-1}$), and foliage density (leaf area index LAI, $\text{m}^2 \text{m}^{-2}$) (Bessagnet et al., 2009). Therefore, for

any given species, the emissions rate (ER, $\mu\text{g m}^{-2} \text{h}^{-1}$) is calculated as a function of an emission factor at canopy standard conditions EF ($\mu\text{g m}^{-2} \text{h}^{-1}$) and an emission activity factor g (unitless) that accounts for deviations from canopy standard conditions (Anav et al., 2011).

2.5. BIOGEOCHEM module

Two biogeochemical models have been included in the MORCE platform: the Eco3M (Baklouti et al., 2006a,b) and PISCES (Aumont et al., 2003) models. The integration of these two models is motivated by the fact that PISCES is a widely used global model that can be implemented easily in various regions of the world while Eco3M integrates the Mediterranean specificities of the Mediterranean ecosystems among which the non-Redfieldian composition of inorganic and organic matter (the Redfield ratio is the molecular ratio of carbon (C), nitrogen (N) and phosphorus (P) in plankton). The comparison and/or combination of the two models will allow global coupled studies with regional focus.

2.5.1. Eco3M model

The Eco3M modeling tool (Baklouti et al., 2006a), developed at LOPB, is a modular tool that handles multi-element multi-functional group biogeochemical models. The mathematical functions for the biogeochemical processes are gathered in a numerical library which is continuously enriched by new functions. These formulations are, for most of them, based on mechanistic considerations. A stage-structured population model of copepods has also been introduced in Eco3M (Eisenhauer et al., 2009).

Eco3M turned out to be particularly suitable for the representation of the pelagic ecosystem of the Mediterranean Sea since it allows to model the planktonic growth submitted to multiple nutrient limitations, the process of diazotrophy and the seasonal planktonic successions. In addition, the implication of the major biogenic elements in the model (C, N, P) and the variable

stoichiometry of the modeled organisms renders possible the reproduction by the model of some specific Mediterranean features such as the high observed N/P ratios or the accumulation of dissolved organic carbon in the surface layer during the stratification period (Auger, 2011). The model will also be used to provide some explanation to the origin of such features, as this has been initiated in Mauriac et al. (2011).

The biogeochemical model used for the MORCE platform encompasses original and mechanistic formulations for the main biogeochemical processes, namely (i) photosynthesis, respiration, chlorophyll synthesis and dissolved organic matter exudation for phytoplankton (Baklouti et al., 2006a), (ii) dissolved organic matter mineralization by bacteria and ammonium and phosphate excretion by zooplankton (Baklouti et al., 2001), (iii) bacterial respiration related to intracellular quotas (Mauriac et al., 2011). In addition to their description in terms of biogenic elements or molecules (C, N, P, Chl, Si) (Chl being Chlorophyll and Si Silicon), organisms are also represented through a cellular (or individual for metazoans) concentration (Mauriac et al., 2011), with the resultant benefits that for each organism, growth and carbon production can be differentiated, that grazing can be better represented (ingestion rate are indeed generally provided in terms of number of preys caught per unit time per unit predator) and that advection of biogeochemical organisms can be easily represented.

2.5.2. PISCES model

The PISCES model (Aumont et al., 2003), developed at Laboratoire de Physique de l'Océan (LPO) and IPSL, is an ecosystem model allowing the simulation of the oceanic carbon cycle. It represents the cycles of dissolved organic carbon, oxygen alkalinity and of five nutritive elements (nitrate, ammonium, phosphate, silicate and iron Fe) which may limit phytoplankton growth (Aumont and Bopp, 2006). Four living compartments are represented: two groups of phytoplankton (diatoms and nanophytoplankton) and two groups of zooplankton (microzooplankton and mesozooplankton). For all species, constant redfield ratios (C/N/P) are imposed, but the C/Si/Fe ratios are variable for phytoplankton. Three compartments are represented nonliving things: dissolved organic carbon semi-labile, small (organic carbon) and coarse particles (calcite, biogenic silica, organic carbon). The two classes of particles are distinguished by their settling velocities and their content is controlled by mortality, grazing and mineralization. The two classes of particulate carbon interact through processes of aggregation and disaggregation (Gehlen et al., 2006). The process of denitrification and nitrogen fixation are also represented. This model has less flexibility than the model Eco3M in terms of diversity of plankton, but can respond to problems on ocean acidification in the event of increased atmospheric carbon dioxide.

3. Coupling

In MORCE platform version 1, the different modules are coupled to each other using two different techniques:

- the OCE and ATM modules are coupled through the OASIS coupler version 3 since complex source grid interpolation and multi-processors computation management are required.
- the LSM is called as subroutines of the ATM and CHEM modules, and the BIOGEOCHEM module is called as subroutine of the OCE module allowing the sharing of the relevant variables on identical numerical grids.

In version 1, the nesting capacity of the MORCE platform to kilometer-scale resolution has not been tested and the runoff does not yet go to the ocean. This latter point requires a coupling

between the LSM and OCE modules and is short-term perspective. The MORCE platform version 1 flow chart is detailed in Fig. 2. The meaning of the names of the variables exchanged between the different modules of the platform in Fig. 2 are given in Table 1.

3.1. ATM/OCE coupling

The coupling between NEMO (OCE) and WRF (ATM) is done with the OASIS version 3 coupler (Valcke, 2006). The coupling frequency, that is the time frequency of the exchanges between ATM and OCE modules, and the interpolation methods are chosen by the user in OASIS ($\Delta t_{\text{CPL}} = \Delta t_{\text{ATM/OCE}}$, see Table 1 and Fig. 2). The coupling frequency $t_{\text{ATM/OCE}}$ is, at least, the largest time step between the OCE and ATM modules. The 6 exchanged variables are the two wind stress components, solar heat flux, non-solar heat flux (net long wave radiation, sensible and latent heat fluxes) and fresh water flux (evaporation minus precipitation) for ATM to OCE, and sea surface temperature (SST) for OCE to ATM. In MORCE platform version 1, the ATM/OCE coupled system is limited to the ocean and the atmosphere compartments, the river runoffs being from climatology.

The ATM/OCE coupling is done with the inclusion of the OASIS version 3 subroutines in each compartment model code source and of its libraries in the makefiles. The OASIS subroutines are split into 4 steps: initialization (opening and reading), definition of partition (mpp computation), exchange (reception and sending) and finalization (restart writing and closing). The heart of the coupling takes place in the surface modules of NEMO and WRF. The reception/sending routines are called at each time-step in the source module (ATM or OCE) but the interpolation by OASIS and the transfer of the "new" fields from the "source" to the "target" module (ATM or OCE) effectively occurs only at the coupling frequency chosen by the user ($\Delta t_{\text{CPL}} = \Delta t_{\text{ATM/OCE}}$). For NEMO, this inclusion of the OASIS subroutines already exists: the compilation before coupling should only include the *key_coupled* and *key_oasis3* and the OASIS libraries. For WRF, subroutines (*module_first_rk_step_part1.F*, *module_dm.F*, *module_io_quilt.F*, *module_wrf_top.F*, *module_surface_driver.F*) have been modified and subroutine *module_cpl_oasis3.F* which acts as an interface with the OASIS coupler, has been added. The makefiles have also been modified. A patch for compiling WRF with OASIS is available on demand to the main author (philippe.drobinski@lmd.polytechnique.fr) until the open-access interface for the full MORCE platform is finalized. Before running the coupled system, the user should finally prepare carefully the OASIS coupling restart files, *namelist (namcouple)* and coupling grid definition (*masks, grids, areas*).

3.2. ATM/LSM coupling

The ORCHIDEE (LSM) land surface scheme has already been implemented in the LMDZ, the atmospheric module of the IPSL global Earth system IPSL-CM (Polcher et al., 1998; Li, 1999; Hourdin et al., 2006). In MORCE, it has also been implemented in the same way as the others land surface model already present in WRF (ATM). The surface atmosphere coupling frequency is the WRF time step $\Delta t_{\text{CPL}} = \Delta t_{\text{ATM}}$. The variables between models are exchanged at high frequency compared to a GCM coupling, compatible with the turbulent processes in the atmospheric model. Indeed, in WRF, $\Delta t_{\text{ATM}} \sim 3-6\Delta x$ where Δt_{ATM} is the time integration in seconds and Δx is WRF horizontal resolution in kilometers. So for $\Delta x \sim 10$ km, $\Delta t \sim 30-60$ s.

In addition to wind, air potential enthalpy, pressure and temperature and air humidity at the lowest level, the ATM module provides the drag coefficient for heat and moisture, as well as the short wave and long wave incoming radiation flux at the surface

(Table 1 and Fig. 2). Precipitation is decomposed into rain and snowfall rate per seconds. Global atmospheric carbon concentration is held constant during the year but can vary from one year to the other.

The ATM module receives in return the albedo, surface roughness, emissivity and sensible heat flux, latent heat flux, evaporation, and runoff split into river runoff and coastal outlet runoff. The heat flux is calculated using bulk aerodynamic formulas. Latent heat is a weighted average between snow sublimation, soil evaporation, canopy transpiration and interception loss. Their variables depend mainly of aerodynamic, canopy, architectural and soil resistance. Albedo and surface roughness are average values over each type of PFT and bare soil. Surface roughness depends on tree height. Constant albedo values are prescribed for each PFT and for bare soil, the albedo depends on soil color and moisture (Wilson and Henderson-Sellers, 1985).

As ORCHIDEE has been designed for a coupling with LMDZ and an off-line usage, the coupling has been straightforward. Inspired by the general surface atmosphere interface prospect in Polcher et al. (1998), the subroutine *intersurf90* of ORCHIDEE and *module_surface_driver.F* of WRF contained the information needed and so the technical implementation was simple. However in contrast to LMDZ, coupling is in an explicit method owing to the shorter time step. Because the two models use different methods to determine the precision of real and integer variables, some adaptation of the makefiles is needed before compilation.

3.3. CHEM/LSM coupling

CHIMERE and ORCHIDEE are coupled via canopy conductance, LAI (Leaf Area Index), and surface ozone concentration, as described in Fig. 2. In order to compute the impact of ozone on photosynthesis and the consequent change in dry deposition, the canopy conductance and surface ozone concentration are exchanged by the models at hourly time step ($\Delta t_{\text{CPL}} = 1$ h, see Table 1 and Fig. 2), while the LAI is used at daily time step to compute biogenic emissions ($\Delta t_{\text{CPL}} = 1$ day, see Table 1 and Fig. 2). In the coupled version, instead of using the multiplicative algorithm developed by Jarvis (1976) to account for canopy conductance, CHIMERE uses the canopy conductance directly computed by ORCHIDEE.

In ORCHIDEE the stomatal conductance parameterization follows the semi-mechanistic model of Ball et al. (1987). This algorithm has become increasingly popular in combination with photosynthesis models (e.g. Farquhar et al., 1980) for plant growth simulations. Since it offers the opportunity to model ozone-induced changes of the photosynthetic rate, it is of interest for ozone impact assessment (e.g. Weinstein et al., 1998). Therefore, this algorithm is well suited to study the feedback between ozone-photosynthesis/canopy conductance-atmospheric chemistry. According to the Ball' et al. (1987) parameterization, the stomatal conductance g_{sto} is directly dependent on the CO_2 concentration (C_s) and the relative humidity (h_s) at the leaf surface, and indirectly dependent on temperature and radiation, via net photosynthesis (A_n):

$$g_{\text{sto}} = g_0 + \frac{kA_n h_s}{C_s} \quad (1)$$

where g_0 is the residual stomatal conductance when A_n approaches zero, k is the slope of the relationship between g_{sto} and the Ball index $A_n h_s / C_s$. For a plant under well-watered conditions k is constant; thus the Ball model is a simple linear relationship between g_{sto} and $A_n h_s / C_s$ (Gutschick and Simonneau, 2002). However, under soil water deficits k has been shown to vary, and the relationship between g_{sto} and the Ball index becomes curvilinear (Sala and Tenhunen, 1996).

ORCHIDEE has been modified to include the effects of ozone on photosynthesis (Anav et al., 2011). The parameterization of ozone impact on the gross primary production (GPP) is based on Felzer et al. (2004). In this formulation ozone is supposed to impact photosynthesis through its concentration in chloroplasts. In the original formulation this concentration is supposed to be dependent on atmospheric concentration and moisture conditions. This latter factor was calculated from the ratio of evapotranspiration to potential evapotranspiration. Since in ORCHIDEE we explicitly compute the stomatal conductance, we modified the original formulation to estimate the ozone impact from stomatal conductance. Then, we assume that chloroplast concentration is proportional to atmospheric concentration and stomatal conductance. Therefore, the instantaneous impact on assimilation ($I_{\text{O}_3, \text{inst}}$ represents the ratio of ozone-exposed to control photosynthesis expressed as a dimensionless value between 0 and 1) is estimated by:

$$I_{\text{O}_3, \text{inst}} = \alpha g_{\text{sto}} \text{AOT}_{40} \quad (2)$$

where g_{sto} is the stomatal conductance (mm s^{-1}), AOT_{40} (Accumulated exposure Over a Threshold of 40 ppb, expressed as ppb h) is the hourly atmospheric ozone concentration over the 40 ppb threshold, and α is an empirically-derived ozone response coefficient (Felzer et al., 2004). In order to account for some persistent damage from past ozone exposure during the lifespan of a leaf, for each month we compute a mean monthly ozone impact ($I_{\text{O}_3, \text{month}}$). This monthly impact is computed from instantaneous ozone impact using the linear relaxation method used in ORCHIDEE to approximate long-term variables (Krinner et al., 2005):

$$I_{\text{O}_3, \text{inst}} = \frac{I_{\text{O}_3, \text{month}} dt_{\text{month}} + I_{\text{O}_3, \text{inst}}}{dt_{\text{month}+1}} \quad (3)$$

where dt_{month} is the number of ORCHIDEE time steps within a month. Therefore, the actual impact of ozone on photosynthesis (I_{O_3}) is defined as:

$$I_{\text{O}_3} = \frac{3I_{\text{O}_3, \text{month}} + I_{\text{O}_3, \text{inst}}}{4} \quad (4)$$

This relative proportion between monthly and instantaneous effect has been empirically computed to fit observed long-term impact of ozone during high exposure levels. Finally we compute the gross primary production as:

$$\text{GPP}_{\text{O}_3} = \text{GPP}(1 - I_{\text{O}_3}) \quad (5)$$

where GPP_{O_3} is the ozone impacted GPP, and GPP is the original photosynthesis calculated by ORCHIDEE.

Technically speaking, few subroutines have been changed in ORCHIDEE and CHIMERE to allow their coupling with CHIMERE. In the appendix, Table 1 summarizes the modifications implemented in the two modules.

3.4. OCE/BIOGEOCHEM coupling

The two ocean biogeochemical modules are coupled with the NEMO system through different ways accounting for the fact that PISCES is part of the NEMO system and that the Eco3M tool is not. In addition, since the biogeochemical model is included in the Eco3M modular platform through a text file, a preliminary compilation is required in order to include the biogeochemical equations in the source files. Both PISCES and Eco3M use the NEMO standard transport equation of passive tracers. In practice, the transport equation for heat and salinity solved by the NEMO numerical model has been extended to the biogeochemical tracers. Different numerical schemes are available for the advection of the passive

tracers. Since Eco3M is a multi-element model (each organism or organic material is represented through several concentrations), these schemes have been adapted in order to handle the advection of non-independent concentrations. These adaptations allow to insure the consistency between the advection of the chemical elements and the advection of the individuals. In addition, the source and sink terms of the biogeochemical tracers (and exclusively due to biogeochemical processes) are provided by the biogeochemical models PISCES or Eco3M.

4. MORCE platform management

Such a unique regional Earth system is a very complex numerical system. Each module of MORCE requires a strong expertise which is ensured in the MORCE development group by the respective module developers. Most of the modules are freely accessible, but only few provide full user support which consists in a detailed documentation, on-line support, user meeting or/and training sessions. In the appendix of the revised article, [Table A.2](#) compiles the references and on-line documentation for the various modules of the MORCE platform.

The MORCE platform is composed of modules, each module is managed independently by its own developers with a separate control version system including documentation. This organization guarantees a sustainable development of each module. The MORCE system has to be easily deployed to the user community and the evolution of the code must be shared between the different developers. The coupling of MORCE modules have shared modifications with patches managed through the same control version system installed in a forge server of IPSL. This is the first step of the management of the MORCE platform version 1.

However, giving public access to the MORCE platform and associated user support is a task requiring significant manpower which is not available for all MORCE modules. As a consequence, the MORCE platform version 1 can not offer a broad public access, so the MORCE control version system repository is not available to public at present. However, mid-term solution for versions higher than version 1 is to produce a detailed documentation and give access to simulations (and if possible the associated code source) performed with already tested and published configurations. This solution should evolve towards full public access at longer-term.

5. MORCE applications: modeling the climate and environment in the Mediterranean and Indian Ocean regions

5.1. Simulations in the Mediterranean region

The Mediterranean region is a particularly vulnerable region featuring an almost-enclosed basin with pronounced orography around its perimeter, a sharply-contrasted climate and heavy urbanization. Interactions and feedback effects between the various domains in this basin play a decisive role in the geophysical and biological dynamics. Forecasting extreme events in the region (such as intense rainfall and flooding in autumn, strong winds and rough seas - whether related or unrelated to the Mediterranean cyclogenesis, droughts and forest fires) is difficult, owing to a lack of information about their preconditioning, which involves a whole range of hierarchically-interlocking coupled processes that act in a non-linear manner at smallest scales. It also the region displaying very large atmospheric aerosol load of natural (mineral dust storms) and human (urban and industrial pollution) origins, as well as high gaseous pollutant concentrations cause by photochemical transformation produced by large solar insolation. The MORCE platform is thus required for a better understanding of the role of this hierarchy in the generation of extreme events in the

Mediterranean region, in order to better assess their predictability and improve forecasting performance, and more generally for identifying the mechanisms underpinning the Mediterranean region's climate in the context of global warming.

Series of simulations have been performed with the different modules of the MORCE platform. For the Mediterranean domain, the ATM module was run with a horizontal resolution of 20 and 30 km for the whole basin, and of 15 km in the zoom (see [Fig. 1](#)). Initial and lateral conditions were taken from the European Center for Medium-range Weather Forecast (ECMWF) ERA-interim reanalysis ([Simons et al., 2007](#)) and from the National Center for Environmental Predictions (NCEP) reanalysis ([Kanamitsu et al., 2002](#)) provided every 6 h with a 0.75° and 2.5° horizontal resolution, respectively. A complete set of physics parameterizations is used which description can be found in [Lebeaupin Brossier et al. \(2011\)](#) and [Anav et al. \(2011\)](#). The CHEM module uses the same grid-resolution as the ATM module and is forced very hour by the ATM module. The initial and boundary conditions are provided by LMDZ-INCA2 chemistry-transport model ([Hauglustaine et al., 2004](#)) and the hourly emissions for the main anthropogenic gas and aerosol species are provided by EMEP ([Vestreng, 2003](#)). The ocean model OCE module has a 1/12° horizontal resolution (about 7 km). The initial conditions for the 3D potential temperature and salinity fields of the OCE module are provided by the MODB4 climatology ([Brankart and Brasseur, 1998](#)) except in the Atlantic zone between 11°W and 5.5°W where the [Levitus et al. \(2005\)](#) climatology is applied. In this area, a 3D relaxation to this monthly climatology is applied during simulations. The runoffs and the Black Sea water input are prescribed from a climatology as localized precipitation ([Beuvier et al., 2010](#)).

5.1.1. Impact of tropospheric ozone on vegetation and consequent changes in biogenic emissions and dry deposition

The MORCE platform has been used in order to improve our knowledge on the regional impact of tropospheric ozone on Euro-Mediterranean vegetation and the consequent changes in biogenic emission and ozone dry deposition owing to modifications in canopy conductance and LAI. Several air pollutants provide an unfavourable condition for vegetation growth and may affect plant's metabolism, ecosystem structure and functions in different ways ([Heagle, 1989](#); [Heagle et al., 1999](#); [Ashmore, 2005](#); [Munifering et al., 2006](#)). Among common air pollutants, O₃ is probably the most damaging to forest vegetation ([Ollinger et al., 1997](#)) and frequently it reaches high concentrations over large regions of the world ([Akimoto, 2003](#); [Vingarzan, 2004](#); [Oltmans et al., 2006](#)). The faster response of plants to O₃ exposure involves essentially changes in stomatal behaviour resulting in a photosynthesis reduction ([Reich, 1987](#); [Wittig et al., 2007](#)) that in turn may lead on longer times to a leaf area index reduction (LAI) ([Anav et al., 2011](#)) that affects both emission ([Guenther et al., 2006](#)) and deposition processes ([Wesely, 1989](#)). Air pollutants may also affect photosynthesis modifying the amount of incident radiation reaching the top of the vegetation canopies ([Bergin et al., 2001](#)). Despite several studies performed to assess the impacts of pollution on vegetation models (e.g. [Adams et al., 1989](#); [Ollinger et al., 1997](#); [Martin et al., 2001](#); [Felzer et al., 2004](#); [Ren et al., 2007](#); [Karnosky et al., 2001, 2007](#); [Nunn et al., 2002, 2005](#); [Werner and Fabian, 2002](#); [Matyssek et al., 2007, 2010a,b](#)), the vegetation-atmosphere feedbacks are still to be investigated.

[Anav et al. \(2011\)](#) used the MORCE platform, without interactive OCE module and using the original Jarvis formulation to estimate the canopy conductance, in order to analyze these feedbacks. Compared to field data, the coupling allows a better estimation of both total and stomatal ozone fluxes of different vegetation types, taking into account both plant phenology and environmental

conditions. The results are shown for year 2002. Fig. 3 displays the simulated inhibitory effect of O_3 on GPP, cumulated over the whole year 2002. This impact has been assessed by performing 2 different simulations with the LSM module (ORCHIDEE): in the first one (control simulation, henceforth CTL), the impact of ozone on the vegetation is not account for, while in the coupled simulation (henceforth MORCE) the impact of ozone on GPP is computed as described in Section 3 and in Anav et al. (2011). The GPP reduction is computed as the difference between the CTL and MORCE simulations. The ozone/vegetation feedbacks induce a significant reduction in GPP, except in North Africa, where the vegetation is absent. The mean reduction is about $200\text{--}300\text{ gC m}^{-2}\text{ yr}^{-1}$ which roughly corresponds to 20–25% of the annual value.

In order to quantify the effect of the coupling on model results, a one-way coupled simulation (henceforth CPL0) has also been performed. It consists in using the ozone data from the CHEM module (CHIMERE) in the LSM module (ORCHIDEE) without accounting for any feedback between the models. In such case, the impact of coupling on model results is computed as the difference between the MORCE and CPL0 simulations (Fig. 3b). The GPP reduction is much more evident in CLP0 experiment than in the MORCE simulation (Fig. 3b). Specifically, in Central-Western Europe the maximum GPP reduction in CPL0 is about $200\text{ gC m}^{-2}\text{ yr}^{-1}$ larger than in MORCE. This behavior is strictly related to the LAI used in the two different CHIMERE simulations that lead to differences in biogenic emissions and hence in the O_3 concentration. The reduction in carbon assimilation also results in a smaller amount of biomass stored and hence to a decrease of LAI. The pattern of LAI decrease matches the location of the maximum GPP decrease (Fig. 3c). It is also noteworthy that the decrease in LAI is much more evident in the CPL0 simulation than in the MORCE simulation (Fig. 3d), since the effect of O_3 on GPP is higher in the CPL0 simulation.

Fig. 4 shows an LAI comparison between the simulations (CTL, CPL0 and MORCE) and the MODIS observations. The monthly LAI time series spatially have been averaged on the PRUDENCE subdomains which are the British Isles (BI), Iberian Peninsula (IP), France (FR), ME (Mid-Europe), Scandinavia (SC), the Alps (AL), the Mediterranean (MD) and East-Europe (EE) (Christensen and Christensen, 2007). Generally the ORCHIDEE results agree with the MODIS observations, without much difference between the CPL0 and MORCE runs. The largest differences occur in the

Scandinavian subdomain (SC), where, during winter, snows cover the canopy mainly composed of evergreen needleleaf forests, leading to an underestimation of LAI measurements with MODIS.

5.1.2. Impact of vegetation on regional water cycle, droughts and heat waves

The 2003 European heat wave was by far the warmest summer on record in Europe, especially in France. The heat wave led to health crises in several countries and combined with drought to create a crop shortfall in Southern Europe. More than 40,000 Europeans died as a result of the heat wave (Robine et al., 2008). Several studies have been carried out on the 2003 summer heat wave, all focusing on the contribution of the various component of the Earth system. Synoptic weather conditions that have been associated to it are the summer atmospheric blocking and the “Atlantic low” regime (Cassou et al., 2005; Beniston and Diaz, 2004; Colacino and Conte, 1995; Fink et al., 2004; Stéfanon et al., in press). SST effects have been explored in several sensitivity studies. It has been established that they can explain half of the observed anomaly and is essential to reproduce all its main features (Feudale and Shukla, 2010; Black et al., 2004; Nakamura et al., 2005). Nevertheless, land as well as boundary conditions are also fundamental. Soil moisture deficit enhances temperature through surface heat and latent fluxes and other indirect local effects (Ferranti and Viterbo, 2006; Fischer et al., 2007; Zampieri et al., 2009).

A comparatively less investigated process is the role of the vegetation on the amplitude of the 2003 summer temperature anomaly. The MORCE platform has been used for this purpose with two different configurations: one control run (CTL) was performed with prescribed leaf area index (LAI) of year 2002, thus limiting the effect of vegetation feedback to stomatal resistance only, and one fully coupled run with freely evolving LAI (MORCE). The results are shown over France (red box in Fig. 1). Fig. 5 exhibits the spatial differences between the MORCE and CTL simulations over the heat wave period (1–15 August 2003). MORCE simulation shows higher temperature (up to $1.5\text{ }^\circ\text{C}$) over most of the domain except over the mountainous region (Massif Central) where it is $1\text{ }^\circ\text{C}$ cooler with respect to the CTL simulation (Fig. 5a). The regions of higher (resp. lower) temperature in the MORCE simulation correspond to the regions where latent heat (i.e. evaporation) is smaller (resp. larger) in the MORCE simulation (Fig. 5b). Due to energy partitioning

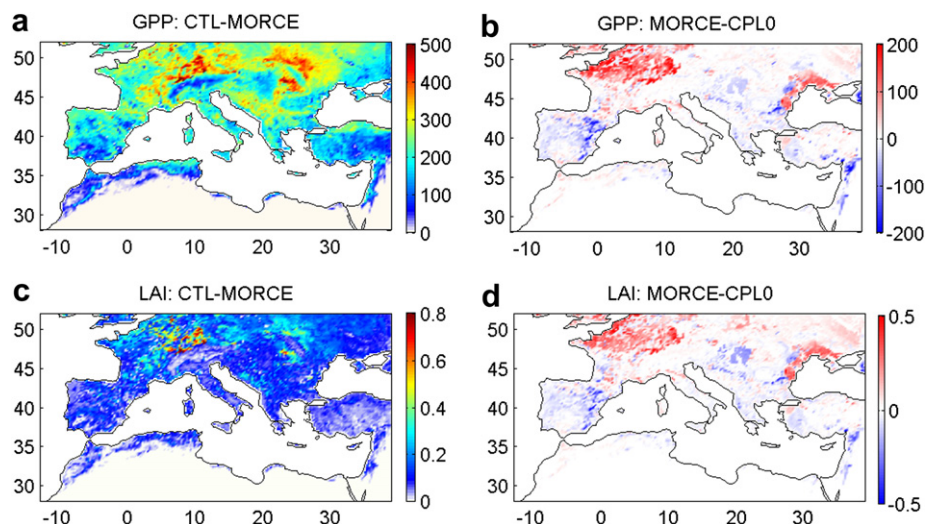


Fig. 3. Upper row: GPP difference between the CTL and MORCE simulations (a) and between the MORCE and CPL0 simulations (in $\text{gC m}^{-2}\text{ yr}^{-1}$); Lower row (panels c and d) is similar to upper row (panels a and b) for LAI (in $\text{m}^2\text{ m}^{-2}$).

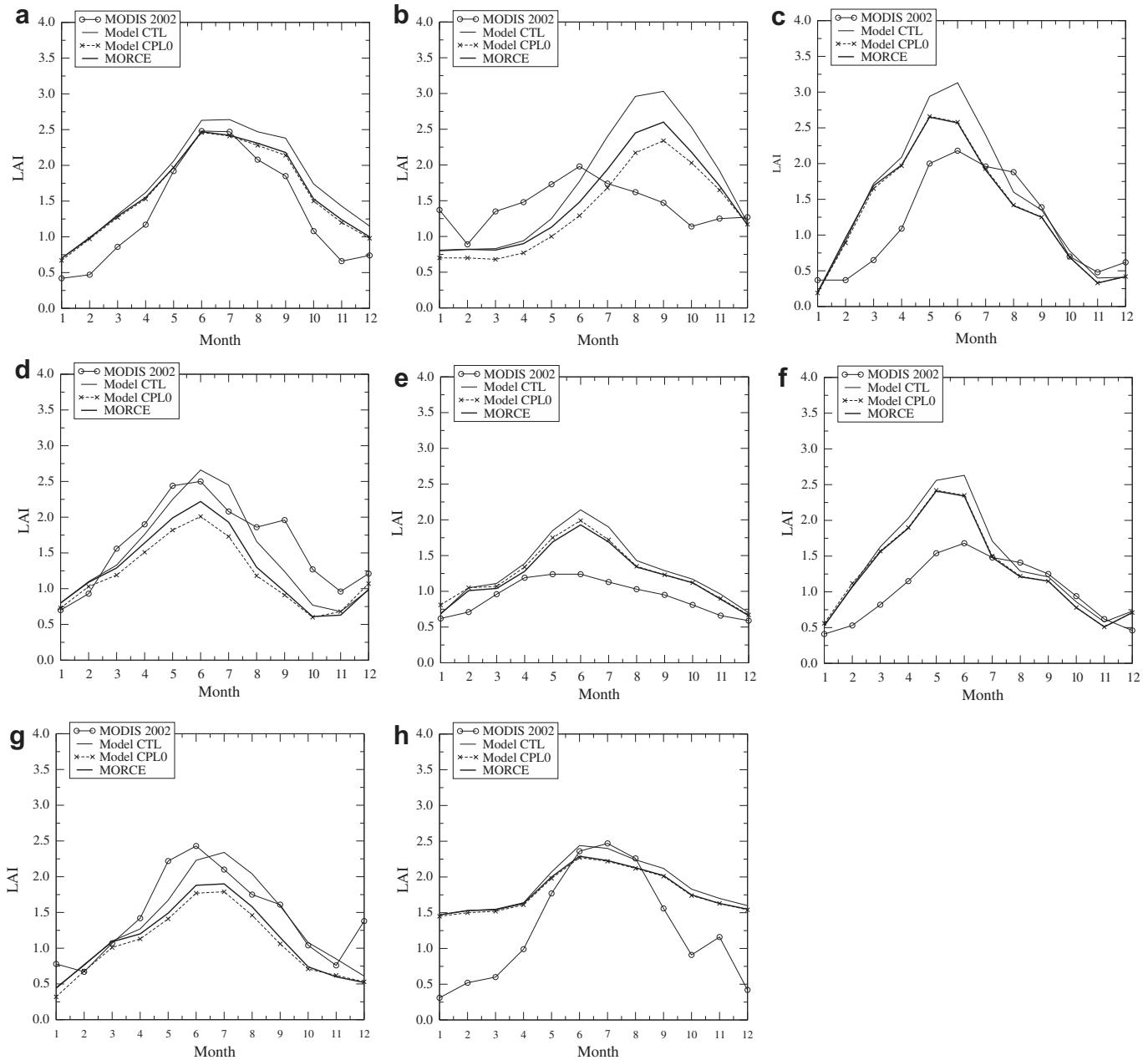


Fig. 4. Monthly LAI time series spatially averaged over the PRUDENCE sub-domains which are AL (a), BI (b), EA (c), FR (d), IP (e), MD (f), ME (g) and SC (h). The circles represent the LAI retrieved from MODIS observations. The thin solid line, the crosses and the thick solid line represent the simulated LAI for the CTL, CPL0 and MORCE simulations, respectively.

between latent and sensible heat, all areas where latent flux decreases implies increasing temperature due to dry convection. As latent heat flux in ORCHIDEE is the weighted average of snow sublimation, soil evaporation, evaporation of foliage water and canopy transpiration, it strongly depends on vegetation processes (Ducoudré et al., 1993). Fig. 5 (panels c and d) show LAI and gross primary production (GPP) anomalies (MORCE-CTL). LAI and GPP are representative of vegetation state. LAI reflects vegetation build-up and growing throughout the year. The amount of vegetation is a partial indicator of the ability to evaporate water from the soil. The areas showing the most significant LAI deficit in the MORCE simulation with respect to the CTL simulation, display the largest positive temperature anomalies and decrease of latent heat flux. Conversely, GPP is an indicator of the instantaneous plant activity, positively correlated to stomatal opening. We find for most of the

domain a decrease in GPP in MORCE simulation with respect to the CTL simulation, associated with larger canopy resistance. Thus, the combination in some areas of a decrease of LAI and GPP is one key factor for sensible heat flux enhancement (or conversely latent heat decrease) and temperature increase.

Comparison of the CTL and MORCE simulations with the European Climate Assessment and Data (ECA&D) gridded dataset (Klein Tank et al., 2002) has been carried out for surface temperature (Fig. 6). The temperature averaged over the simulation domain is 35.49 °C for the CTL run, 35.89 °C for the MORCE run and 35.46 °C for ECA&D. The spatial pattern is fairly similar between the two simulations. The MORCE simulation overestimates the surface temperature by about 2 °C in the South Western part of the domain but is very close to the gridded data in the Northern part of the domain. The CTL simulation is too cold by about 2 °C in the

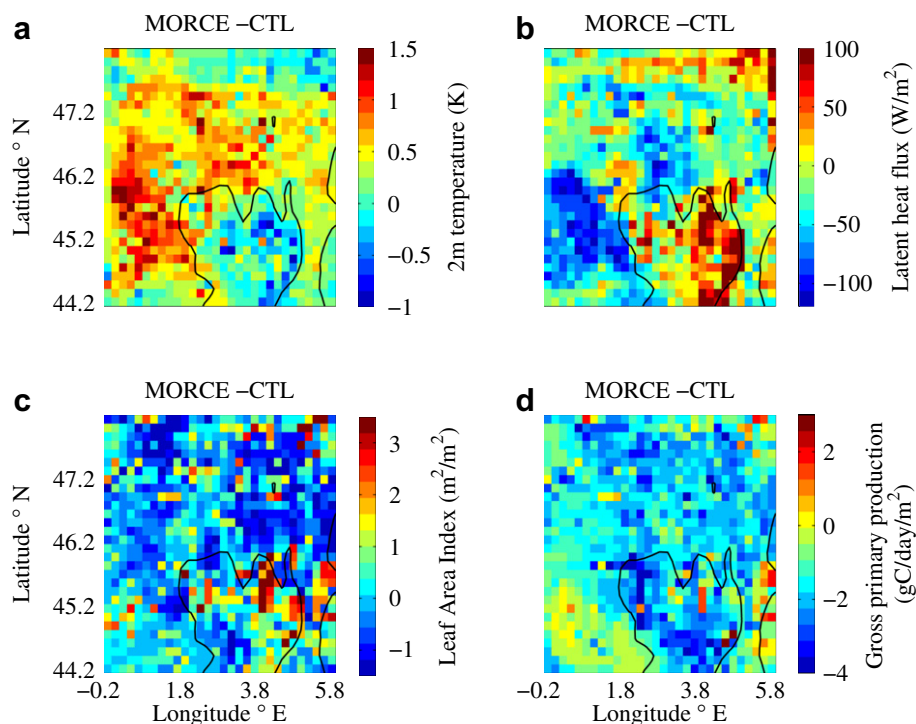


Fig. 5. Difference between the MORCE and CTL simulations over the domain indicated by a red box in Fig. 1 for (a) 2-m temperature, (b) latent heat flux (positive when latent heat is released into the atmosphere), (c) leaf area index (LAI) and (d) gross primary production (GPP). The variables are averages at 1200 UTC over the heat wave period (1–15 August 2003). The solid black line indicates the 500-m terrain height. (For interpretation of the references to colour in this figure legend, the reader is referred to the web version of this article.)

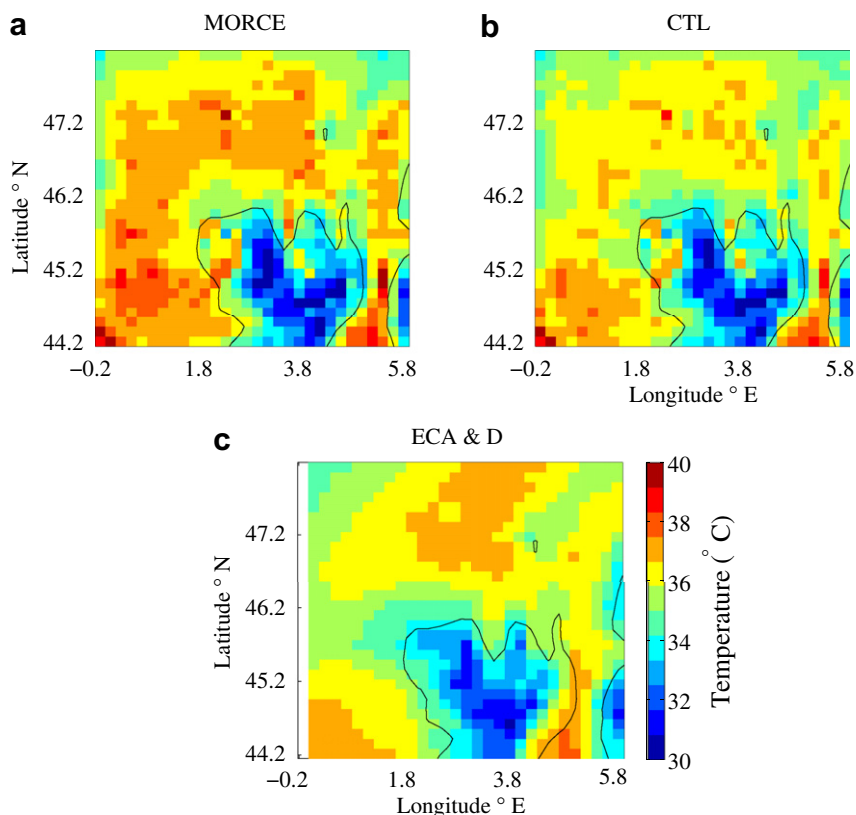


Fig. 6. Surface temperature field average over the first 15 days of August 2003 from the MORCE simulation (a), the CTL simulation (b) and ECA&D gridded dataset (c).

Northern part of the domain and close to the observations in the South Western part of the domain.

5.1.3. Role of ocean/atmosphere interactions and feedbacks on thermohaline circulation and meteorological extremes

The Mediterranean Sea water budget (evaporation–precipitation) is a relevant integrated proxy to investigate the regional water cycle at the various time scales with the integration of the contribution of all Earth compartments. It is also suited to evaluate the contribution of mesoscale coupled processes on the regional climate. Lebeauvin Brossier et al. (2011) already showed WRF model's ability to well represent the fresh water budget.

To quantify the effect of coupled processes, 20-year simulations (1989–2008) using the atmosphere-only module (i.e. WRF at 20 km resolution being forced by ERA-interim reanalyzed SST; hereafter referred as the CTL simulation) and the MORCE platform (i.e. coupled with NEMO at 6–8 km resolution – Lebeauvin Brossier et al., 2011; Beuquier et al., submitted for publication; hereafter referred as the MORCE simulation) have been performed in the context of the HyMeX program (Drobinski et al., 2009a,b; 2010) and the CORDEX program (Giorgi et al., 2009). In HyMeX and CORDEX, only the coupling between the ATM and OCE modules has been considered. We analyze precipitation (P) and evaporation (E) budgets (runoff is not considered in our experiments). E is strongly related to SST and wind speed via bulk formulae and is

consequently directly modified by the coupling. P is indirectly related to the surface and is more a signature of the coupling impact on the atmospheric model physics.

The differences between the CTL and MORCE simulations are analyzed in terms of evaporation (E), precipitation (P) and budget (E–P) (Fig. 7). The difference between the two simulations are expressed as relative anomaly with respect to CTL run (in %). Compared to CTL, the MORCE SST of the Mediterranean Sea is more accurately predicted (not shown). The MORCE platform produces mesoscale patterns of ≈ 40 km diameter in SST and turbulent fluxes fields that are not present in CTL. The wind speed is weaker in the MORCE simulation over the whole domain (-1.7% on average), except over some SST hot-spots (not shown). Weaker winds in ocean-atmosphere coupled simulations have already been evidenced by Pullen et al. (2006) over the Adriatic Sea due to SST stabilizing effect. In the ATM module, the SST modifications induce strong feedbacks on P and E fields. The P anomaly is locally significant with values between $-75\%/+50\%$ (Fig. 7a), and the E anomaly is between $-50\%/+60\%$ (Fig. 7c). We found a significant spatial correspondence between the SST anomaly and the P and E anomalies: correlation coefficients calculated over the Mediterranean Sea are 0.76 for P and 0.97 for E. Over the rest of the domain, the decrease in E is linked to the weaker winds. The P anomaly displays very small patterns which extend over the coastal area. However, the extension seems to be limited to the strong

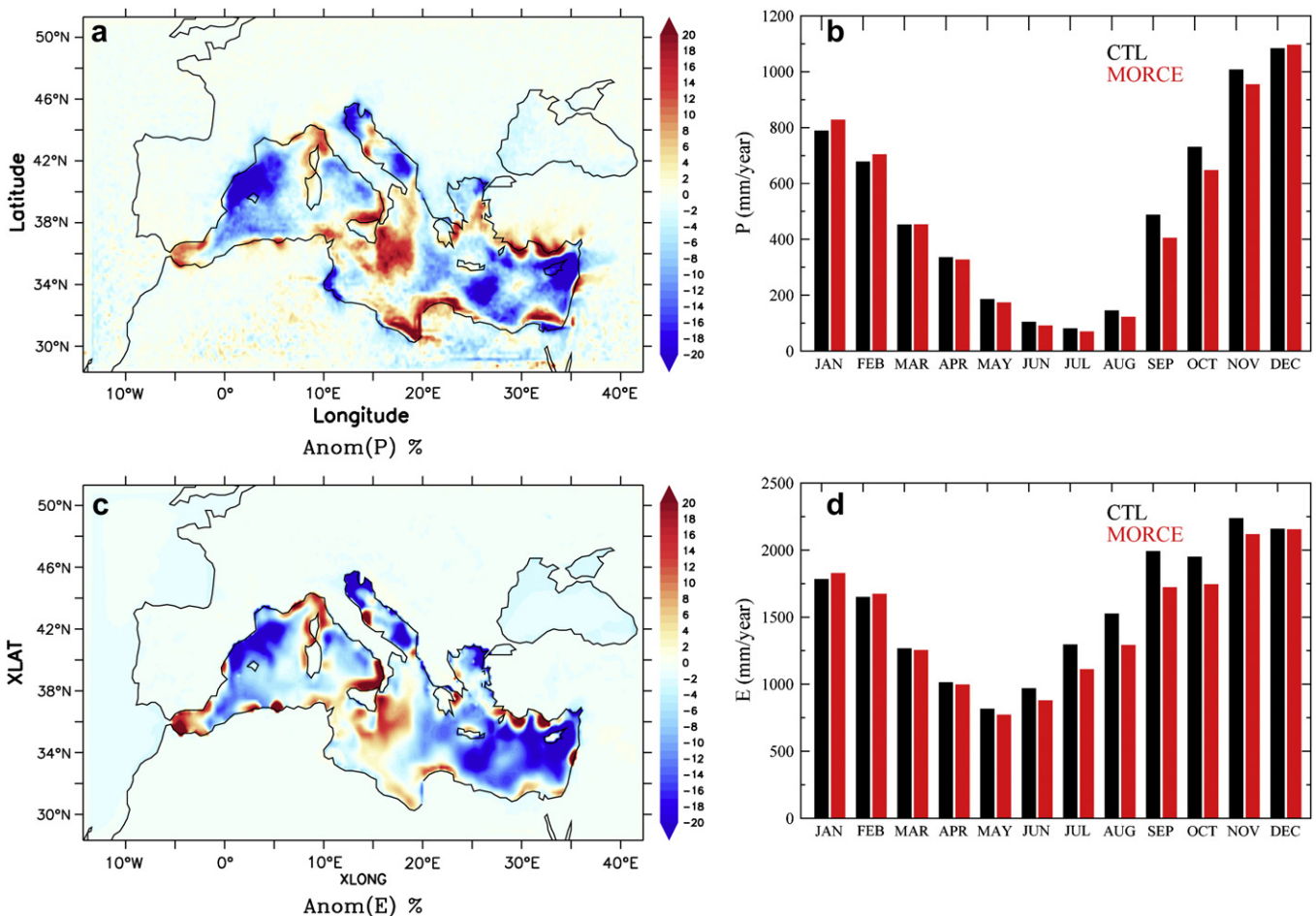


Fig. 7. Left panels: Relative difference between MORCE and CTL simulations with respect to the CTL simulation for (a) precipitation P and (c) evaporation E over 1989–2008 period. Right panels: Composites over 1989–2008 of the annual cycle for (b) precipitation P and (d) evaporation E over the whole Mediterranean Sea in the CTL (black) and MORCE (red) simulations. (For interpretation of the references to colour in this figure legend, the reader is referred to the web version of this article.)

surrounding topography. Finally, the spatial average of these anomalies are small (-1% for P and -1.5% for E over the whole domain; -3% for P and -5% for E over the Mediterranean Sea).

Looking at the annual variability over the sea (Fig. 7b,d), small differences are found for both P and E. P and E are slightly larger in Winter in MORCE than in CTL simulation, and are smaller in Fall. The Mediterranean Sea budgets (E–P) are finally 1.05 m yr^{-1} in CTL and 0.97 m yr^{-1} in MORCE. Table 2 gives for comparison the P and E estimates derived from observations (in-situ measurements and satellite products) over the Mediterranean Sea with the associated article references. The E estimates range between 1121 and 1570 mm yr^{-1} (40% variability), whereas the P estimates range between 292 and 700 mm yr^{-1} (140% variability). The E and P estimates with CTL and MORCE outputs are within the range of the observed estimates. These large ranges of variability evidences the difficulty to produce accurate estimates of evaporation and precipitation over the Mediterranean Sea, due both to the coarse spatial and temporal resolutions of the measurements and the “small” size of the Mediterranean Sea which prevents reliable satellite products over the coastal regions and the Adriatic Sea (e.g. Romanou et al., 2010). These data thus highlight the main challenge of the coming years, i.e. the production of E and P estimates with improved accuracy to quantify the contribution of the coupled processes in the Mediterranean Sea water budget, and to evaluate ocean-atmosphere coupled models. This is one central objective of the HyMeX program (Drobinski et al., 2009a,b, 2010).

Finally, this comparison highlights that ocean-atmosphere coupled processes play major role in redistributing “water” at mesoscale over the Mediterranean Sea with key spots.

5.2. Simulations in the Indian Ocean

The MORCE platform is also deployed over the tropical and subtropical Indian Ocean region. Its main objective is to provide a well-adapted tool to study the link between oceanic variability and cyclonic activity in this region. Indeed, one third of the world population lives in the coastal regions surrounding the Indian Ocean. These regions are highly vulnerable to the extreme events such as heavy flooding and strong winds associated with tropical cyclones and monsoon depressions. This cyclonic activity represents about 27% of the global cyclonic activity with an average of 22 tropical storms (wind $>17.5 \text{ m s}^{-1}$, i.e. 34 knots) and 10 tropical

cyclones (wind $>32.9 \text{ m s}^{-1}$, i.e. 64 knots) per year. Unfortunately, the strong variability of these meteorological phenomena is still poorly understood in the Indian Ocean for different reasons. First, tropical storms are synoptic-scale phenomena needing relatively high spatial resolution to be well represented in numerical models. The physical processes associated with these tropical systems cover a broad range of temporal and spatial atmospheric scales, which are difficult to fully assess. Second, the evolution of individual storms (track and intensity) depends on large-scale environment characteristics such as wind shear, and on the sea surface temperature and heat content of the Indian Ocean.

Given these constrains, the MORCE platform has been used to realistically represent tropical systems structure and mesoscale oceanic features. The configuration set-up has a uniform spatial resolution of $1/4^\circ$ for both ATM and OCE modules. The initial and lateral conditions of the ATM module are provided by the ERA-Interim reanalysis. The OCE module uses a climatological initial state with no current provided by Levitus et al. (2005). Boundaries conditions are provided by a global forced oceanic run named ORCAO25-G70. It covers the entire period with a spatial resolution of $1/4^\circ$. This global simulation was driven without data assimilation by the hybrid interannual forcing DFS3 described in Brodeau et al. (2010). The influence of air-sea coupling on tropical cyclones characteristics is assessed by performing a sensitivity experiment where a control simulation (hereafter referred as CTL simulation) using the ATM module is forced by the sea surface temperature produced by the MORCE simulation over the 1990–2009 period. Comparing the CTL and MORCE simulations allows us identifying how the air-sea coupling under tropical cyclones modulates the statistics of the simulated cyclonic activity in each region. Differences in number and spatial distribution of cyclogenesis between the CTL and MORCE simulations are presented in Fig. 8. Regarding the location of the cyclogenesis in the South Indian Ocean, a clear meridional shift appeared when comparing the 2 simulations. In the CTL simulation, the main formation zone is located close to the equator, while the main development region extends more poleward in the MORCE simulation. The number and the annual cycle of the cyclogenesis is also strongly affected by the coupling with the ocean (Fig. 8b). In the CTL simulation, the annual mean number of cyclogenesis is 70% higher than in the MORCE simulation. The analysis of the climatological seasonal cycle reveals that this difference comes mainly from the January–March season which is the main development period in the southern hemisphere. When compared to observations (IBTrACS database; Knapp et al., 2010), the cyclogenesis seasonal cycle is reasonably well reproduced by both simulations. But the MORCE simulation shows a better agreement with observations in terms of number of tropical cyclones per year due to the coupling with the ocean (Fig. 8b). These preliminary results based on the MORCE platform shows a promising potential to achieve a better understanding of the air-sea coupling influence on the Indian cyclonic activity.

6. Perspectives

Version 1 of the MORCE platform has already proved its usefulness for a deep insight in coupled processes and their contribution to regional climate variability. In particular, the MORCE platform is used within the CORDEX program of WCRP regional downscaling experiment (Giorgi et al., 2009), with a special focus over the Mediterranean in the framework of the HyMeX (e.g. Drobinski et al., 2009a,b, 2010) and MED-CORDEX (Ruti et al., submitted for publication). In this context, the MORCE platform has been used to downscale ERA-interim reanalysis (1989–2008) as part of phase 1 of the CORDEX program, and thorough evaluation of the MORCE platform is on-going. The first

Table 2

Comparison to published previous estimates from observations (in-situ measurements and satellite products) of precipitation (P) and evaporation (E) over the Mediterranean Sea.

| Reference | Method | E (mm/yr) | P (mm/yr) |
|----------------------------|--|-----------|-----------|
| Carter (1956) | Measurements of Mertz (1918) | 1160 | 410 |
| Tixeront (1970) | Observations from coastal stations | 1200 | 350 |
| Bunker (1972) | SSMO data | 1570 | |
| Ovchinnikov (1974) | Measurements | 1250 | 400 |
| Jaeger (1976) | Measurements | 1210 | 550 |
| Béthoux (1979) | Marine advection and meteorological survey | 1540 | 310 |
| Gilman and Garrett (1994) | Derived from in-situ observations | 1121–1430 | 550–700 |
| Castellari et al. (1998) | Derived from in-situ observations | 1320–1570 | 550–700 |
| Béthoux and Gentili (1999) | Derived from in-situ observations | 1360–1540 | 310 |
| Mehta and Yang (2008) | TRMM products | | 360–700 |
| Romanou et al. (2010) | HOAPS3 products | 1037 | 292 |
| This study | CTL simulation | 1533 | 499 |
| | MORCE simulation | 1442 | 482 |

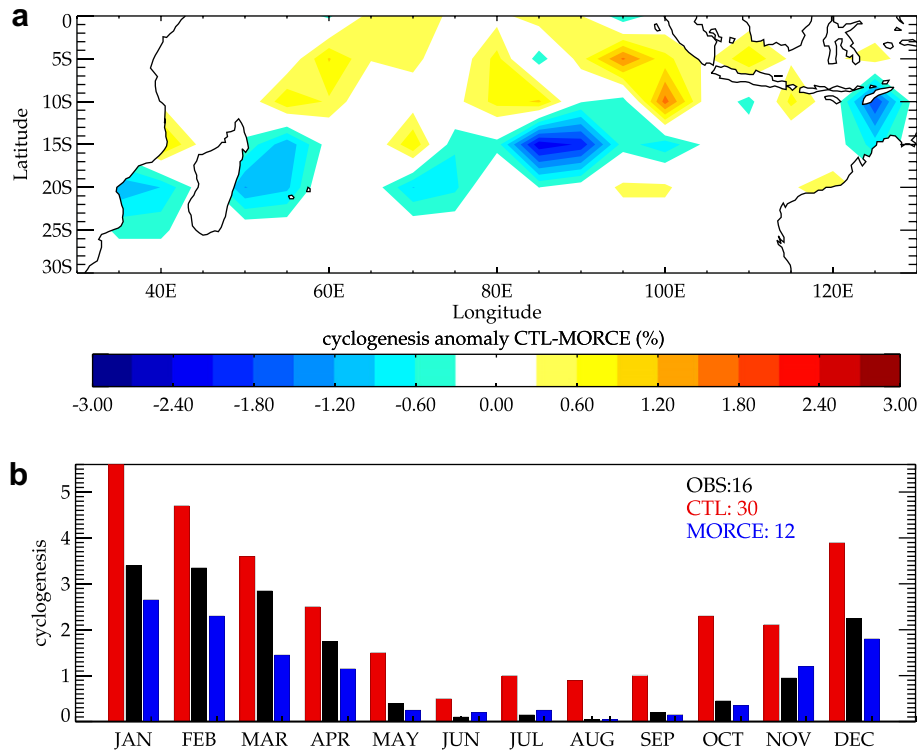


Fig. 8. Differences in the spatial distribution of cyclogenesis (a) and the number of cyclones (b) between the CTL (blue bars) and MORCE (red bars) simulations, and IBTrACS observations (black bars). (For interpretation of the references to colour in this figure legend, the reader is referred to the web version of this article.)

studies conducted with the MORCE platform has focused on ocean/atmosphere coupled processes on the Mediterranean Sea water budget and on the extreme events (intense winds and precipitation) in the Mediterranean (not shown in this paper) and over the Indian Ocean. It has also been used to investigate the impact of vegetation/chemistry/hydrology coupling on vegetation evolution and associated impact on water cycle (and droughts and heat waves in particular) and the impact of the water cycle in the Mediterranean region.

As a follow-up of phase 1 of the CORDEX program, the downscaling of simulations performed in the frame of the Coupled Model Intercomparison Project No. 5 (CMIP5) simulations for emission scenario RCP4.5 and RCP8.5 (RCP standing for Representative Concentration Pathways) has just started in the frame of CORDEX phase 2 to investigate the evolution (variability and trend) of the Mediterranean regional climate.

The perspectives for version 2 of the MORCE platform are to couple:

1. the ATM and CHEM modules to include the interactions between atmospheric composition, radiative budget and nucleation processes
2. the LSM and OCE modules to include river runoff into the ocean (which is a key issue for the Mediterranean area)
3. the CHEM module to the BIOGEOCHEM module, to include the role of aerosols deposition on the sea surface as nutrients for marine pelagic ecosystems.

and to integrate in WRF the physical parameterization of the IPSL global circulation model LMDZ (Hourdin et al., 2006) to improve the physics consistency when using the MORCE platform for downscaling the IPSL global Earth Simulator IPSL-CM (all other modules of MORCE platform are common with IPSL-CM). The grid

nesting capacity in all compartments which is a key added value of such a regional modeling platform will be tested in the near-future.

Acknowledgments

This work has mainly been conducted in the IPSL group for regional climate and environment studies. It received support was funded by GIS (Groupement d'Intérêt Scientifique) "Climat, Environnement et Société". It also received support from ANR CHAMPION (Vagues de CHaleur d'été: Mécanismes, Prévisibilité, Impacts) project, FP7 CIRCE (Climate Change and Impact Research: the Mediterranean Environment) and IS-ENES (InfraStructure for the European Network for the Earth System Modelling) projects. This work also contributes to the HyMeX program (HYdrological cycle in The Mediterranean EXperiment) through INSU-MISTRALS support and the CORDEX program (A COordinated Regional climate Downscaling EXperiment). This work was granted access to the HPC resources of IDRIS (Institut du Développement et des Ressources en Informatique Scientifique) of the Centre National de la Recherche Scientifique (CNRS) under allocation 2009 (i2009010227) and 2011 (i2011010227) made by the Grand Equipement National de Calcul Intensif (GENCI). The authors are grateful to SiMED and GLORYS projects funded by Mercator, and in particular to Charles Deltel from LOCEAN/IPSL, Florent Lyard from LEGOS, Wolfgang Ludwig from CEFREM, Nicolas Ferry and Yann Drillet from Mercator Ocean and Bernard Barnier from LEGI, for their help for developing the Mediterranean Sea configuration of the NEMO model.

Appendix A

Table A.1: Summarizes the modifications implemented in the CHEM and LSM modules for their coupling.

Table A.1. List of modified routines in CHIMERE and ORCHIDEE for their coupling.

| List of modified subroutines in ORCHIDEE | Function |
|--|--|
| <i>dim2_driver.f90</i> (main) | Allow the synchronization with CHIMERE |
| <i>readdim2.f90</i> | Read the ozone data provided by CHIMERE |
| <i>intersurf.f90</i> | Pass the O ₃ array to ORCHIDEE (SECHIBA) subroutines |
| <i>difffuco.f90</i> | Compute the ozone stress |
| <i>constantes_co2.f90</i> | Contains the ozone sensitivity parameters for the different vegetation types |
| List of modified subroutines in CHIMERE | Function |
| <i>chimere.sh</i> (main script) | Add flags to enable/disable the coupling |
| <i>chimere-emis.sh</i> | Write a namelist used by CHIMERE for biogenic emissions |
| <i>chimere-init.sh</i> | Contains all the model initializations |
| <i>chimere-run.sh</i> | Write a namelist used by CHIMERE for the coupling |
| <i>diagbio.f90, diagbio_megan.f90</i> | Use the ORCHIDEE LAI to compute biogenic emissions |
| <i>diagbio_common.f90</i> | |
| <i>chimere.f90</i> (main) | Used for model synchronization |
| <i>worker_common.f90, worker_message_subs.f90</i> | Contain variables declarations and MPI calls |
| <i>chimere_common.f90, master_message_subs.f90</i> | |
| <i>message_defs.f90</i> | |
| <i>iniparam.f90</i> | Adds the original CHIMERE canopy conductance in the outputs |
| <i>outprint.f90</i> | Saves the original CHIMERE canopy conductance in the outputs |
| <i>iniread.f90</i> | Retrieves the netcdf id code of ORCHIDEE canopy conductance |
| <i>readhour.f90</i> | Reads the hourly ORCHIDEE canopy conductance |
| <i>depvel.f90</i> | Compute dry deposition using the ORCHIDEE canopy conductance |
| <i>integrun.f90</i> | Hourly synchronization with ORCHIDEE |
| List of added subroutines in CHIMERE | Function |
| <i>start_orchidee.f90, chimere_orchidee.f90</i> | Used to generate a script to submit and run ORCHIDEE and read the data |
| <i>get_orchidee_canopy.f90</i> | |

Table A.2: Compiles the references, the web site address where the codes of the various modules of the MORCE platform can be downloaded and the on-line documentation can be found.

Table A.2: Documentation of the various MORCE modules.

| Module | Model | On-line documentation | Main references |
|------------|----------|---|-------------------------|
| ATM | WRF | http://www.wrf-model.org/ | Skamarock et al. (2008) |
| CHEM | CHIMERE | http://www/lmd.polytechnique.fr/chimere | Bessagnet et al. (2009) |
| OCE | NEMO | http://www.nemo-ocean.eu/ | Madec (2008) |
| BIOGEOCHEM | PISCES | http://www.lodyc.jussieu.fr/aumont/pisces.html | Aumont et al. (2003) |
| BIOGEOCHEM | Eco3M | http://www.com.univ-mrs.fr/LOB/spip.php?article208 | Baklouti et al., 2006a |
| LSM | ORCHIDEE | http://orchidee.ipsl.jussieu.fr/ | Krinner et al. (2005) |
| Coupler | OASIS | https://verc.enes.org/models/software-tools/oasis/ | Valcke (2006) |

References

- Adams, R.M., Glycer, D.J., Johnson, S.L., McCarl, B.A., 1989. A reassessment of the economic effects of ozone on United States agriculture. *J. Air Waste Manage. Assoc.* 39, 960968.
- Akimoto, H., 2003. Global air quality and pollution. *Science* 302, 1716–1719.
- Aldrian, E., Sein, D., Jacob, D., Dümenil Gates, L., Podzun, R., 2005. Modeling Indonesian rainfall with a coupled regional model. *Clim. Dyn.* 25, 1–17.
- Alpert, P., Stein, U., Tsidulko, M., 1995. Role of sea fluxes and topography in eastern Mediterranean cyclogenesis. In: *The Global Atmosphere and Ocean System*, vol. 3, pp. 55–79.
- Anav, A., Menut, L., Khvorostyanov, D., Viovy, N., 2011. Impact of tropospheric ozone on the Euro-Mediterranean vegetation. *Glob. Change Biol.* 17. doi:10.1111/j.1365-2486.2010.02387.x.
- Arora, V., 2002. Modeling vegetation as a dynamic component in soil-vegetation-atmosphere transfer schemes and hydrological models. *Rev. Geophys.* 40, 1006. doi:10.1029/2001RG000103.
- Artale, V., Calmanti, S., Carillo, A., Dell'Aquila, A., Herrmann, M., Pisacane, G., Ruti, P.M., Sannino, G., Struglia, M.V., Giorgi, F., Bi, X., Pal, J.S., Rauscher, S., 2009. An atmosphereocean regional climate model for the Mediterranean area: assessment of a present climate simulation. *Clim. Dyn.* 35, 721–740.
- Ashmore, M.R., 2005. Assessing the future global impacts of ozone on vegetation. *Plant Cell Environ.* 28, 949–964.
- Auger, P.A., 2011. Modélisation des écosystèmes planctoniques pélagiques en Méditerranée nord-occidentale. Impact des eaux du Rhône l'échelle du plateau du Golfe du Lion et variabilité interannuelle à décennale au large. (Ecole Doctorale n°173). PhD. thesis. Université Paul Sabatier, Toulouse, 242 pp.
- Aumont, O., Bopp, L., 2006. Globalizing results from ocean in situ iron fertilization studies. *Glob. Biogeochem. Cy.* 20, GB2017. doi:10.1029/2005GB002591.
- Aumont, O., Maier-Reimer, E., Blain, S., Pondaven, P., 2003. An ecosystem model of the global ocean including Fe, Si, P co-limitations. *Glob. Biogeochem. Cy.* 17, 1060. doi:10.1029/2001GB001745.
- Baklouti, M., Chevalier, C., Bouvy, M., Corbin, D., Pagano, Troussellier, M., Arfi, R., 2001. A study of plankton dynamics under osmotic stress in an estuary (Senegal River) using a 3D mechanistic model. *Prog. Oceanogr.* 222, 2704–2721.
- Baklouti, M., Diaz, F., Pinazo, C., Faure, V., Queguiner, B., 2006a. Investigation of mechanistic formulations depicting phytoplankton dynamics for models of marine pelagic ecosystems and description of a new model. *Prog. Oceanogr.* 71, 1–33.
- Baklouti, M., Faure, V., Pawlowski, L., Sciandra, A., 2006b. Investigation and sensitivity analysis of a mechanistic phytoplankton model implemented in a new modular numerical tool (Eco3M) dedicated to biogeochemical modelling. *Prog. Oceanogr.* 71, 34–58.
- Ball, J.T., Woodrow, I.E., Berry, J.A., 1987. A model predicting stomatal conductance and its contribution to the control of photosynthesis under different environmental conditions. In: Biggens, J. (Ed.), *Progress in Photosynthesis Research*, vol. IV. Martinus Nijhoff, Dordrecht, pp. 221–224.
- Beniston, M., Diaz, H., 2004. The 2003 heat wave as an example of summer in a greenhouse climate? Observations and climate model simulations for Basel, Switzerland. *Glob. Planet. Change* 44, 73–81.
- Bergin, M.H., Cass, G.H., Xu, J., Fang, C., Zeng, L.M., Yu, T., Salmon, L.G., Kiang, C.S., Tang, X.Y., Zhang, Y.H., Chameides, W.L., 2001. Aerosol radiative, physical and chemical properties during June 1999. *J. Geophys. Res.* 106, 17969–17980.
- Bessagnet, B., Menut, L., Aymoz, G., Chepfer, H., Vautard, R., 2008. Modelling dust emissions and transport within Europe: the Ukraine March 2007 event. *J. Geophys. Res.* 113, D15202. doi:10.1029/2007JD009541.
- Bessagnet, B., Menut, L., Curci, G., Hodzic, A., Guillaume, B., Liousse, C., Moukhtar, S., Pun, B., Seigneur, C., Schulz, M., 2009. Regional modeling of carbonaceous aerosols over Europe - Focus on secondary organic aerosols. *J. Atmos. Chem.* 61, 175–202.
- Bessagnet, B., Seigneur, C., Menut, L., 2010. Impact of dry deposition of semi-volatile organic compounds on secondary organic aerosols. *Atmos. Env.* 44, 1781–1787.
- Béthoux, J.P., 1979. Budgets of the Mediterranean Sea: their dependence on the local climate and on the characteristics of the Atlantic waters. *Oceanol. Acta* 2, 105–119.

- Béthoux, J.P., Gentili, B., 1999. Functioning of the Mediterranean Sea: past and present changes related to freshwater input and climatic changes. *J. Mar. Syst.* 20, 33–47.
- Beuvier, J., Sevault, F., Herrmann, M., Kontoyiannis, H., Ludwig, W., Rixen, M., Stanev, E., Béranger, K., Somot, S., 2010. Modelling the Mediterranean Sea interannual variability during 1961–2000: focus on the eastern Mediterranean Transient (EMT). *J. Geophys. Res.* 115, C08517. doi:10.1029/2009JC005850.
- Beuvier, J., Branger, K., Lebeaupin Brossier, C., Bourdallé-Badie, R., Sevault, F., Somot, S., Drillet, Y., Ferry, N., Lyard, F., submitted for publication. Spreading of the Western Mediterranean Deep Water after winter 2005: time-scales and deep cyclones transport. *J. Geophys. Res.*
- Black, E., Balckburn, M., Harrison, G., Hoskins, B., Methven, J., 2004. Factors contributing to the summer 2003 European heat wave. *Weather* 59, 217–221.
- Bozec, A., Bouruet-Aubertot, P., Ludicone, D., Crépon, M., 2008. Impact of penetrative solar flux on water mass transformation in the Mediterranean Sea. *J. Geophys. Res.* 113, C06012. doi:10.1029/2007JC004606.
- Brankart, J.M., Brasseur, P., 1998. The general circulation in the Mediterranean Sea: a climatological approach. *J. Mar. Syst.* 18, 41–70.
- Brodeau, L., Barnier, B., Treguier, A., Penduff, T., Gulev, S., 2010. An ERA40-based atmospheric forcing for global ocean circulation models. *Ocean Model.* 31, 88–104.
- Bunker, A.F., 1972. Wintertime interactions of the atmosphere with the Mediterranean Sea. *J. Phys. Oceanogr.* 2, 225–238.
- Carter, D.B., 1956. The Water Balance of the Mediterranean and Black Seas, vol. 9. Publ. In Climatol. 123–174.
- Cassou, C., Terray, L., Phillips, A.S., 2005. Tropical Atlantic influence on European heat waves. *J. Clim.* 18, 2805–2811.
- Castellari, S., Pinardi, N., Leaman, K., 1998. A model study of air-sea interactions in the Mediterranean Sea. *J. Mar. Syst.* 18, 89–114.
- Christensen, J.H., Christensen, O.B., 2007. A summary of the PRUDENCE model projections of changes in European climate by the end of this century. *Climatic Change* 81, 7–30.
- Colacino, M., Conte, M., 1995. Heat waves in the Central Mediterranean. A synoptic climatology. *Il Nuovo Cimento* 18, 295–304.
- Collatz, G., Ribas-Carbo, M., Berry, J., 1992. Coupled photosynthesis-stomatal conductance model for leaves of C plants. *Aust. J. Plant Physiol.* 19, 519–538.
- Crétat, J., Pohl, B., Richard, Y., Drobinski, P., 2011. Uncertainties in simulating regional climate of Southern Africa: sensitivity to physical parameterizations using WRF. *Clim. Dyn.* doi:10.1007/s00382-011-1055-8.
- de Rosnay, P., Polcher, J., 1998. Modeling root water uptake in a complex land surface scheme coupled to a GCM. *Hydrol. Earth Syst. Sci.* 2, 239–256.
- de Rosnay, P., Polcher, J., Laval, K., Sabre, M., 2003. Integrated parameterization of irrigation in the land surface model ORCHIDEE. Validation over the Indian Peninsula. *Geophys. Res. Lett.* 30, 1986. doi:10.1029/2003GL018024.
- Debreu, L., Vouland, C., Blayo, E., 2008. Agrif: adaptive grid refinement in fortran. *Comput. Geosciences* 34, 813.
- Döscher, R., Willén, U., Jones, C., Rutgersson, A., Meier, H.E.M., Hansson, U., 2002. The development of the coupled ocean-atmosphere model RCAO. *Boreal Environ. Res.* 7, 183–192.
- Drobinski, P., Flamant, C., Dusek, J., Flamant, P.H., Pelon, J., 2001. Observational evidence and modeling of an internal hydraulic jump at the atmospheric boundary layer top during a tramontane event. *Boundary-Layer Meteorol.* 98, 497–515.
- Drobinski, P., Bastin, S., Guénard, V., Caccia, J.L., Dabas, A.M., Delville, P., Protat, A., Reitebuch, O., Werner, C., 2005. Summer mistral at the exit of the Rhône valley. *Q. J. R. Meteorol. Soc.* 131, 353–375.
- Drobinski, P., Ducrocq, V., Lionello, P., The HyMeX ISSC, 2009a. HyMeX, a potential new CEOP RHP in the Mediterranean basin. *GEWEX Newsletter* 19, 5–6.
- Drobinski, P., Béranger, K., Ducrocq, V., Allen, J.T., Chronis, G., Font, J., Maded, G., Papatthanassiou, E., Pinardi, N., Sammari, C., Taupier-Letage, I., 2009b. The HyMeX (Hydrological in the Mediterranean Experiment) program: the specific context of oceanography. *MERCATOR Newsletter* 32, 3–4.
- Drobinski, P., Ducrocq, V., Lionello, P., 2010. Studying the hydrological cycle in the Mediterranean. *EOS. Trans. Amer. Geophys. Union* 91, 373.
- Ducoudré, N., Laval, K., Perrier, A., 1993. SECHIBA, a new set of parametrizations of the hydrologic exchanges at the land/atmosphere interface within the LMD atmospheric general circulation model. *J. Clim.* 6, 248–273.
- Ducrocq, V., Nuisser, O., Ricard, D., Lebeaupin, C., Anquetin, S., 2008. A numerical study of three catastrophic precipitating events over Southern France. II: mesoscale triggering and stationarity factors. *Q. J. R. Meteorol. Soc.* 134, 131–145.
- Dulac, F., 2011. The chemistry-aerosol Mediterranean experiment (ChArMEx) initiative. MedCLIVAR final conference, Lecce, Italie.
- d'Orgeval, T., Polcher, J., de Rosnay, P., 2008. Sensitivity of the West African hydrological cycle in ORCHIDEE to infiltration processes. *Hydrol. Earth Syst. Sci.* 12, 1387–1401.
- Eisenhauer, L., Carlotti, F., Baklouti, M., Diaz, F., 2009. Zooplankton population model coupled to a biogeochemical model of the North Western Mediterranean Sea ecosystem. *Ecol. Model.* 220, 2865–2876.
- Farquhar, G.D., Von Caemmerer, S., Berry, J.A., 1980. A biochemical model of photosynthetic CO₂ assimilation in leaves of C₃ species. *Planta* 149, 78–90.
- Felzer, B.S., Kicklighter, D., Melillo, J., Wang, C., Zhuang, Q., Prinn, R., 2004. Effects of ozone on net primary production and carbon sequestration in the conterminous United States using a biogeochemistry model. *Tellus* 56, 230–248.
- Ferranti, L., Viterbo, P., 2006. Sensitivity to soil water initial conditions. *J. Clim.* 19, 3659–3680.
- Feudale, L., Shukla, J., 2010. Influence of sea surface temperature on the European heat wave of 2003 summer. Part II: a modeling study. *Clim. Dyn.* 36, 1705–1715.
- Fink, A.H., Brucher, T., Krüger, A., Leckebush, G.C., Pinto, J.G., Ulbrich, U., 2004. The 2003 European summer heat wave and drought synoptic diagnosis and impacts. *Weather* 59, 209–216.
- Fischer, E.M., Seneviratne, S.I., Luthi, D., Schär, C., 2007. The contribution of land-atmosphere coupling to recent European summer heatwaves. *Geophys. Res. Lett.* 34, L06707. doi:10.1029/2006GL029068.
- Flaounas, E., Bastin, S., Janicot, S., 2010. Regional climate modelling of the 2006 West African monsoon: sensitivity to convection and planetary boundary layer parameterisation using WRF. *Clim. Dyn.* 36, 1083–1105.
- Foley, J.A., Kutzbach, J.E., Coe, M.T., Levis, S., 1994. Feedbacks between climate and boreal forests during the Holocene epoch. *Nature* 371, 52–54.
- Gehlen, M., Bopp, L., Emprin, N., Aumont, O., Heinze, C., Ragueneau, O., 2006. Reconciling surface ocean productivity, export fluxes and sediment composition in a global biogeochemical ocean model. *Biogeosciences* 3, 521–537.
- Gilman, C., Garrett, C., 1994. Heat flux parameterizations for the Mediterranean Sea: the role of atmospheric aerosols and constraints from the water budget. *J. Geophys. Res.* 99, 5119–5134.
- Giorgi, F., 2006a. Regional climate modeling: status and perspectives. *J. Phys.* 139, 101–118.
- Giorgi, F., 2006b. Climate change hot-spots. *Geophys. Res. Lett.* 33, L08707. doi:10.1029/2006GL025734.
- Giorgi, F., Jones, C., Asrar, G.R., 2009. Addressing climate information needs at the regional level: the CORDEX framework. *WMO Bull.* 58, 175–183.
- Guénard, V., Drobinski, P., Caccia, J.L., Campistron, B., Bénéch, B., 2005. An observational study of the mesoscale mistral dynamics. *Boundary-Layer Meteorol.* 115, 263–288.
- Guénard, V., Drobinski, P., Caccia, J.L., Tedeschi, G., Currier, P., 2006. Dynamics of the MAP IOP-15 severe mistral event: observations and high-resolution numerical simulations. *Q. J. R. Meteorol. Soc.* 132, 757–778.
- Guenther, A., Karl, T., Harley, P., Wiedinmyer, C., Palmer, P.L., Geron, C., 2006. Estimates of global terrestrial isoprene emissions using MEGAN (Model of Emissions of Gases and Aerosols from Nature). *Atmos. Chem. Phys.* 6, 3181–3210.
- Gutschick, V.P., Simonneau, T., 2002. Modelling stomatal conductance of fieldgrown sunflower under varying soil water content and leaf environment: comparison of three models of stomatal response to leaf environment and coupling with an abscisic acid-based model of stomatal response to soil drying. *Plant Cell Environ.* 25, 1423–1434.
- Hauglustaine, D.A., Hourdin, F., Jourdain, L., Filiberti, M.A., Walters, S., Lamarque, J.F., Holland, E.A., 2004. Interactive chemistry in the Laboratoire de Météorologie Dynamique general circulation model: description and background tropospheric chemistry evaluation. *J. Geophys. Res.* 109. doi:10.1029/2003JD003957.
- Heagle, A.S., 1989. Ozone and crop yield. *Ann. Rev. Phytopathology* 27, 397–423.
- Heagle, A.S., Mille, J.S., Booker, F.L., Pursley, W.A., 1999. Ozone stress, carbon dioxide enrichment, and nitrogen fertility interactions in cotton. *Crop Sci.* 39, 731–741.
- Hourdin, F., Musat, I., Bony, S., Braconnot, P., Codron, F., Dufresne, J.L., Fairhead, L., Filiberti, M.A., Friedlingstein, P., Grandpeix, J.Y., Krinner, G., LeVan, P., Li, Z.X., Lott, F., 2006. The LMDZ4 general circulation model: climate performance and sensitivity to parametrized physics with emphasis on tropical convection. *Clim. Dyn.* 27, 787–813.
- IPCC, 2007. Climate change 2007: the physical science basis. In: Solomon, S., Qin, D., Manning, M., Chen, Z., Marquis, M., Averyt, K.B., Tignor, M., Miller, H.L. (Eds.), Contribution of Working Group I to the Fourth Assessment Report of the Intergovernmental Panel on Climate Change. Cambridge University Press, Cambridge, UK, New York, USA.
- Jaeger, L., 1976. Monatskartendes Niederschlags für die ganze Erde. *Ber. Dtsch. Wetterdienstes* 18, 1–38.
- Jarvis, P.G., 1976. The interpretation of the variations in leaf water potential and stomatal conductance found in canopies in the field. *Philosophical Trans. Royal Soc. London B* 273, 593–610.
- Kanamitsu, M., Ebisuzaki, W., Woollen, J., Yang, S.K., Hnilo, J.J., Fiorino, M., Potter, G.L., 2002. NCEP-DEO AMIP-II reanalysis (R-2). *Bull. Amer. Meteorol. Soc.* 83, 1631–1643.
- Karnosky, D.F., Gielen, B., Ceulemans, R., Schlesinger, W.H., Norby, R.J., Oksanen, E., Matussek, R., Hendrey, G.R., 2001. FACE systems for studying the impacts of greenhouse gases on Forest Ecosystems. In: Karnosky, D.F., Scarascia-Mugnozza, G., Ceulemans, R., Innes, J.L. (Eds.), The Impacts of Carbon Dioxide and Other Green-house Gases on Forest Ecosystems. CABI Press, Vienna, pp. 297–324.
- Karnosky, D.F., Werner, H., Holopainen, T., Percy, K., Oksanen, T., Oksanen, E., Heerdt, C., Fabian, P., Nagy, J., Heilman, W., Cox, R., Nelson, N., Matussek, R., 2007. Free-air exposure systems to scale up ozone research to mature trees. *Plant Biol.* 9, 181–190.
- Klein Tank, A.M.G., Wijngaard, J.B., Können, G.P., Böhm, R., Demarée, G., Gocheva, A., Mileta, M., Pashiardis, S., Hejkrlik, L., Kern-Hansen, C., Heino, R., Bessemoulin, P., Müller-Westermeier, G., Tzanakou, M., Szalai, S., Palsdottir, T., Fitzgerald, D., Rubin, S., Capaldo, M., Maugeri, M., Leitass, A., Bukantis, A., Aberfeld, R., Van Engelen, A.F.V., Forland, E., Miletus, M., Coelho, F., Mares, C., Razuvaev, V., Nieplova, E., Cegnar, T., Lopez, J.A., Dahlström, B., Moberg, A., Kirchhofer, W., Ceylan, A., Pachaliuk, O., Alexander, L.V., Petrovic, P., 2002. Daily dataset of 20th-century surface air temperature and precipitation series for the European climate assessment. *Int. J. Climatol.* 22, 1441–1453.
- Knapp, K.R., Kruk, M.C., Levinson, D.H., Diamond, H.J., Neumann, C.J., 2010. The international Best track archive for climate Stewardship (IBTrACS): unifying tropical cyclone best track data. *Bull. Amer. Meteorol. Soc.* 91, 363–376.

- Krinner, G., Viovy, N., De Noblet-Ducoudré, N., Ogée, J., Polcher, J., Friedlingstein, P., Ciais, P., Sitch, S., Colin Prentice, I., 2005. A dynamic global vegetation model for studies of the coupled atmosphere-biosphere system. *Glob. Biogeochem. Cy.* 19, 1–33.
- Lathiere, J., Hauglustaine, D.A., Friend, A., De Noblet-Ducoudré, N., Viovy, N., Folberth, G., 2006. Impact of climate variability and land use change on global biogenic volatile organic compounds emissions. *Atmos. Chem. Phys.* 6, 2129–2146.
- Lebeauin Brossier, C., Drobinski, P., 2009. Numerical high-resolution air-sea coupling over the Gulf of Lions during two Tramontane/Mistral events. *J. Geophys. Res.* 114, D10110. doi:10.1029/2008JD011601.
- Lebeauin Brossier, C., Ducrocq, V., Giordani, H., 2009. Two-way one-dimensional high-resolution air-sea coupled modelling applied to Mediterranean heavy rain events. *Q. J. R. Meteorol. Soc.* 135, 187–204.
- Lebeauin Brossier, C., Béranger, K., Deltel, C., Drobinski, P., 2011. The Mediterranean response to different space-time resolution atmospheric forcings using perpetual mode sensitivity simulations. *Ocean Model.* 36, 1–25.
- Lebeauin, C., Ducrocq, V., Giordani, H., 2006. Sensitivity of Mediterranean torrential rain events to the sea surface temperature based on high-resolution numerical forecasts. *J. Geophys. Res.* 111, D12110. doi:10.1029/2005JD006541.
- Lehmann, A., Lorenz, P., Jacob, D., 2004. Modelling the exceptional Baltic Sea inflow events in 2002–2003. *Geophys. Res. Lett.* 31, L21308. doi:10.1029/2004GL020830.
- Levitus, S., Antonov, J.I., Boyer, T.P., 2005. Warming of the world ocean. *Geophys. Res. Lett.* 32, L02604. doi:10.1029/2004GL021592.
- Li, Z.X., 1999. Ensemble atmospheric GCM simulation of climate interannual variability from 1979 to 1994. *J. Clim.* 12, 986–1001.
- Madec, G., 2008. NEMO Ocean Engine. Note du Pole de modélisation. Institut Pierre-Simon Laplace (IPSL), France. No 27 ISSN No 1288–1619.
- Marshall, J., Adcroft, A., Hill, C., Perelman, L., Heisey, C., 1997a. A finite-volume, incompressible Navier Stokes model for, studies of the ocean on parallel computers. *J. Geophys. Res.* 102, 5753–5766.
- Marshall, J., Hill, C., Perelman, L., Adcroft, A., 1997b. Hydrostatic, quasi-hydrostatic, and nonhydrostatic ocean modeling. *J. Geophys. Res.* 102, 5733–5752.
- Martin, M.J., Host, G.E., Lenz, K.E., 2001. Stimulating the growth response of aspen to elevated ozone: a mechanistic approach to scaling a leaf-level model of ozone effects on photosynthesis to a complex canopy architecture. *Environ. Pollut.* 115, 425–436.
- Matyssek, R., Bahnweg, G., Ceulemans, R., Fabian, P., Grill, D., Hanke, D.E., Kraigher, H., Osswald, W., Rennenberg, H., Sandermann, H., Tausz, M., Wieser, G., 2007. Synopsis of the CASIROZ case study: carbon sink strength of *Fagus sylvatica* L. in a changing environment experimental risk assessment of mitigation by chronic ozone impact. *Plant Biol.* 9, 163–180.
- Matyssek, R., Karnosky, D.F., Wieser, G., Percy, K., Oksanen, E., Grams, T.E., Kusbiske, M., Hanke, D., Pretzsch, H., 2010a. Advances in understanding ozone impact on forest trees: messages from novel phytotron and free-air fumigation studies. *Environ. Pollut.* 158, 1990–2006.
- Matyssek, R., Wieser, G., Ceulemans, R., Rennenberg, H., Pretzsch, H., Haberer, K., Löw, M., Nunn, A.J., Werner, H., Wipfler, P., Osswald, W., Nikolova, P., Hanke, D.E., Kraigher, H., Tausz, M., Bahnweg, G., Kitao, M., Dieler, J., Sandermann, H., Herbinger, K., Grebenc, T., Blumenröther, M., Deckmyn, G., Grams, T.E., Heerd, C., Leuchner, M., Fabian, P., Häberle, K.H., 2010b. Enhanced ozone strongly reduces carbon sink strength of adult beech (*Fagus sylvatica*) – Resume from the free-air fumigation study at Kranzberg Forest. *Environ. Pollut.* 158, 2527–2532.
- Mauriac, R., Moutin, T., Baklouti, M., 2011. Accumulation of DOC in Low Phosphate Low Chlorophyll (LPLC) area: is it related to higher production under high N:P ratio? *Biogeosciences* 8, 933–950.
- Meehl, G.A., 1994. Coupled land–ocean–atmosphere processes and South Asian monsoon variability. *Science* 266, 263–267.
- Mehta, A.V., Yang, S., 2008. Precipitation climatology over Mediterranean basin from ten years of TRMM measurements. *Adv. Geosci.* 17, 87–91.
- Mellor, G.L., 2004. A three-dimensional, primitive equation, numerical ocean model. In: Program in Atmospheric and Oceanic Sciences. Princeton University, Princeton.
- Menut, L., Bessagnet, B., 2010. Atmospheric composition forecasting in Europe. *Ann. Geophys.* 28, 61–74.
- Muntifering, R.B., Chappelka, A.H., Lin, J.C., Karnosky, D.F., Somers, G.L., 2006. Chemical composition and digestibility of Trifolium exposed to elevated ozone and carbon dioxide in a free-air (FACE) fumigation system. *Funct. Ecol.* 20, 269–275.
- Nakamura, M., Enomoto, T., Yamane, S., 2005. A simulation study of the 2003 heatwave in Europe. *J. Earth Simulator* 2, 55–69.
- Nenes, A., Pilinis, C., Pandis, S.N., 1998. ISORROPIA: a new thermodynamic model for inorganic multicomponent atmospheric aerosols. *Aquatic Geochem.* 4, 123–152.
- Nunn, A.J., Reiter, I.M., Häberle, K.H., Werner, H., Langebartsels, C., Sandermann, H., Heerd, C., Fabian, P., Matyssek, R., 2002. “Free-air” ozone canopy fumigation in an old-growth mixed forest: concept and observations in beech. *Phyton* 42, 105–119.
- Nunn, A.J., Kozovits, A.R., Reiter, I.M., Heerd, C., Leuchner, M., Lütz, C., Liu, X., Lo, W.M., Winkler, J.B., Grams, T.E., Häberle, K.H., Werner, H., Fabian, P., Rennenberg, H., Matyssek, R., 2005. Comparison of ozone uptake and responsiveness between a phytotron study with young and a field experiment with adult beech (*Fagus sylvatica*). *Environ. Pollut.* 137, 494506.
- Ollinger, S.V., Aber, J.D., Reich, P.B., 1997. Simulating ozone effects on forest productivity: interactions among leaf-, canopy-, and stand-level processes. *Ecol. Appl.* 7, 1237–1251.
- Oltmans, S.J., Lefohn, A.S., Harris, J.M., Galbally, I., Scheel, H.E., Bodeker, G., Brunke, E., Claude, H., Tarasick, D., Johnson, B.J., Simmonds, P., Shadwick, D., Anlauf, K., Hayden, K., Schmidlin, F., Fujimoto, T., Akagi, K., Meyer, C., Nichol, S., Davies, J., Redondas, A., Cuevas, E., 2006. Long-term changes in tropospheric ozone. *Atmos. Env.* 40, 3156–3173.
- Ovchinnikov, I.M., 1974. On the water balance of the Mediterranean Sea. *Oceanology* 14, 198–202.
- Pal, J.S., Giorgi, F., Bi, X., Elguindi, N., Solmon, F., Gao, X., Rauscher, S.A., Francisco, R., Zakey, A., Winter, J., Ashfaq, M., Syed, F.S., Bell, J.L., Diffenbaugh, N.S., Karmacharya, J., Konaré, A., Martínez, D., da Rocha, R.P., Sloan, L.C., Steiner, A.L., 2007. Regional climate modeling for the developing world: the ICTP RegCM3 and RegCM3. *Bull. Am. Meteorol. Soc.* 88, 1395–1409.
- Petroff, A., Mailliat, A., Amielh, M., Anselmetti, F., 2008. Aerosol dry deposition on vegetative canopies. Part I: review of present knowledge. *Atmos. Env.* 42, 3625–3653.
- Pielke, R.A., Avissar, R., Raupach, M., Dolman, H., Zeng, X., Denning, S., 1998. Interactions between the atmosphere and terrestrial ecosystems: influence on weather and climate. *Glob. Change Biol.* 4, 101–115.
- Polcher, J., McAvaney, B., Viterbo, P., Gaertner, M.A., Hahmann, A., Mahfouf, J.F., Noilhan, J., Phillips, T., Pitman, A., Schlosser, C.A., Schulz, J.P., Timbal, B., Verseghy, D., Xue, Y., 1998. A proposal for a general interface between land-surface schemes and general circulation models. *Glob. Planet. Change* 19, 263–278.
- Prentice, I.C., Heimann, M., Sitch, S., 2000. The carbon balance of the terrestrial biosphere: ecosystem models and atmospheric observations. *Ecol. Appl.* 10, 1553–1573.
- Pullen, J., Doyle, J.D., Signell, R.P., 2006. Two-way air-sea coupling: a study over the Adriatic. *Mon. Wea. Rev.* 134, 1465–1480.
- Ratnam, J.V., Giorgi, F., Kaginalkar, A., Cozzini, S., 2008. Simulation of the Indian monsoon using the RegCM3-ROMS regional coupled model. *Clim. Dyn.* 33, 119–139.
- Reich, P.B., 1987. Quantifying plant response to ozone: a unifying theory. *Tree Physiol.* 3, 63–91.
- Ren, W., Tian, H., Liu, M., et al., 2007. Effects of tropospheric ozone pollution on net primary productivity and carbon storage in terrestrial ecosystems of China. *J. Geophys. Res.* 112, 1–17.
- Rinke, A., Gerdes, R., Dethloff, K., Kandlbinder, T., Karcher, M., Kauker, F., Frickenhaus, S.K., “oberle, C., Hiller, W., 2003. A case study of the anomalous Arctic sea ice conditions during 1990: insights from coupled and uncoupled regional climate model simulations. *J. Geophys. Res.* 108, 4275. doi:10.1029/2002JD003146.
- Robine, J.M., Cheung, S.L.K., Le Roy, S., Van Oyen, H., Griffiths, C., Michel, J.P., Herrmann, F.R., 2008. Death toll exceeded 46,000 in Europe during the summer of 2003. *Comptes Rendus Biologies* 331, 171178.
- Romanou, A., Tselioudis, G., Zerefos, C.S., Clayson, C.A., Curry, J.A., Andersson, A., 2010. Evaporation-Precipitation variability over the Mediterranean and Black Seas from satellite and reanalysis estimates. *J. Clim.* 23, 5268–5287.
- Roulet, G., Madec, G., 2000. Salt conservation, free surface and varying levels: a new formulation for ocean general circulation models. *J. Geophys. Res.* 105, 23927–23942.
- Ruti, P., Somot, S., Dubois, C., Calmanti, S., Ahrens, B., Aznar, R., Bartholy, J., Béranger, K., Bastin, S., Brauch, J., Calvet, J.C., Carillo, A., Alias, A., Decharme, B., Dell’Aquila, A., Djurdjevic, V., Drobinski, P., Elizalde Arellano, A., Gaertner, M., Galan, P., Gallardo, C., Giorgi, F., Gualdi, S., Bellucci, A., Harzallah, A., Herrmann, M., Jacob, D., Khodayar, S., Krichak, S., Lebeauin, C., Lheveder, B., Li, L., Liguori, G., Lionello, P., Baris, O., Rajkovic, B., Sevault, F., Sannino, G., MED-CORDEX initiative for Mediterranean climate studies. *Bull. Amer. Meteorol. Soc.*, submitted for publication.
- Sala, A., Tenhunen, J.D., 1996. Simulations of canopy net photosynthesis and transpiration in Quercus ilex L. under the influence of seasonal drought. *Agric. For. Meteorol.* 78, 203–222.
- Salameh, T., Drobinski, P., Dubos, T., 2010. The effect of indiscriminate nudging time on large and small scales in regional climate modelling: application to the Mediterranean basin. *Q. J. R. Meteorol. Soc.* 136, 170–182.
- Schaap, M., Vautard, R., Bergstrom, R., van Loon, M., Bessagnet, B., Brandt, J., Christensen, H., Cuvelier, K., Foltescu, V., Graff, A., Jonson, J.E., Kerschbaumer, A., Krol, M., Langner, J., Roberts, P., Rouil, L., Stern, R., Tarrason, L., Thunis, P., Vignati, E., White, L., Wind, P., Builtjes, P.H.J., 2007. Evaluation of long-term aerosol simulations from seven air quality models and their ensemble in the EURODELTA study. *Atmos. Env.* 41, 2083–2097.
- Schmidt, H., Derognat, C., Vautard, R., Beekmann, M., 2001. A comparison of simulated and observed O₃ mixing ratios for the summer of 1998 in Western Europe. *Atmos. Env.* 35, 6277–6297.
- Simons, A., Uppala, S., Dee, D., Kobayashi, S., 2007. ERA-interim: New ECMWF reanalysis products from 1989 onwards. *ECMWF Newsletter* 110, 25–35.
- Sitch, S., Smith, B., Prentice, I.C., Arneth, A., Bondeau, A., Cramer, W., Kaplan, J., Levis, S., Lucht, W., Sykes, M., Thonicke, K., Venevski, S., 2003. Evaluation of ecosystem dynamics, plant geography and terrestrial carbon cycling in the LPJ Dynamic Vegetation Model. *Glob. Change Biol.* 9, 161–185.
- Skamarock, W.C., Klemp, J.B., Dudhia, J., Gill, D.O., Barker, D.M., Duda, M.G., Huang, X.-Y.W., Wang Powers, J.G., 2008. A description of the advanced research WRF Version 3, 125 pp., NCAR Technical Note NCAR/TN-475+STR.

- Somot, S., Sevault, F., Déqué, M., 2006. Transient climate change scenario simulation of the Mediterranean Sea for the 21st century using a high-resolution ocean circulation model. *Clim. Dyn.* 27, 851–879.
- Somot, S., Sevault, F., Déqué, M., Crépon, M., 2008. 21st Century climate change scenario for the Mediterranean using a coupled atmosphere-ocean regional climate model. *Glob. Planet Change* 63, 112–126.
- Stéfanon, M., D'Andrea, F., Drobinski, P., Heatwave classification over Europe and the Mediterranean region. *Env. Res. Lett.*, in press.
- The MerMex Group, Durrieu de Madron, X., Guieu, C., Sempéré, R., Conan, P., Cossa, D., D'Ortenzio, F., Estournel, C., Gazeau, F., Rabouille, C., Stemmann, L., Bonnet, S., Diaz, F., Koubbi, P., Radakovitch, O., Babin, M., Baklouti, M., Bancon-Montigny, C., Belviso, S., Bensoussan, N., Bonsang, B., Bouloubassi, I., Brunet, C., Cadiou, J.F., Carlotti, F., Chami, M., Charmasson, S., Charrière, B., Dachsa, J., Doxaran, D., Dutay, J.C., Elbaz-Poulicheta, F., Eléaume, M., Eyrolles, F., Fernandez, C., Fowler, S., Francoua, P., Gaertner, J.C., Galzin, R., Gasparini, S., Ghiglione, J.F., Gonzalez, J.L., Goyet, C., Guidi, L., Guiziana, K., Heimbürger, L.E., Jacquet, S.H.M., Jeffrey, W.H., Joux, F., Le Hir, P., Leblanc, K., Lefèvre, D., Lejeune, C., Lemé, R., Loye-Pilota, M.D., Mallet, M., Méjanella, L., Mélin, F., Mellon, C., Mérigot, B., Merle, P.L., Migon, C., Miller, W.L., Mortier, L., Mostajira, B., Mousseau, L., Moutin, T., Para, J., Pérez, T., Petrenko, A., Poggiale, J.C., Prieur, L., Pujo-Pay, M., Pulido-Villena, V., Raimbault, P., Rees, A.P., Ridame, C., Rontani, J.F., Ruiz Pino, D., Sicre, M.A., Taillandier, V., Tamburini, C., Tanaka, T., Taupier-Letage, I., Tedetti, M., Testor, P., Thébaud, H., Thouvenin, B., Touratier, F., Tronczynski, J., Ulses, C., Van Wambeke, F., Vantrepotte, V., Vaza, S., Verney, R., 2011. Marine ecosystems' responses to climatic and anthropogenic forcings in the Mediterranean. *Prog. Oceanogr.* 91, 97–166.
- Tixeront, J., 1970. Le bilan hydrologique de la mer Noire et de la mer Méditerranée. *Cah. Oceanogr* 3, 227–237.
- Valari, M., Menut, L., 2010. Transferring the heterogeneity of surface emissions to variability in pollutant concentrations over urban areas through a chemistry transport model. *Atmos. Env* 44, 3229–3238.
- Valcke, S., 2006. OASIS3 user guide (prism_2–5) CERFACS technical support, TR/CMGC/06/73, PRISM report No 3, Toulouse, France, 60 pp.
- Van Loon, M., Vautard, R., Schaap, M., Bergstrom, R., Bessagnet, B., Brandt, J., Builtjes, P.J.H., Christensen, J.H., Cuvelier, K., Graf, A., Jonson, J.E., Krol, M., Langner, J., Roberts, P., Rouil, L., Stern, R., Tarrason, L., Thunis, P., Vignati, E., White, L., Wind, P., 2007. Evaluation of long-term ozone simulations from seven regional air quality models and their ensemble average. *Atmos. Env.* 41, 2083–2097.
- Vautard, R., Martin, D., Beekmann, M., Drobinski, P., Friedrich, R., Jaubertie, A., Kley, D., Lattuati, M., Moral, P., Neisinger, B., Theloke, J., 2003. Paris emission inventory diagnostics from the ESQUIF airborne measurements and a chemistry-transport model. *J. Geophys. Res.* 108, 8564., doi:10.1029/2002JD002797.
- Vautard, R., Bessagnet, B., Chin, M., Menut, L., 2005. On the contribution of natural Aeolian sources to particulate matter concentrations in Europe: testing hypotheses with a modelling approach. *Atmos. Env.* 39, 3291–3303.
- Vautard, R., Builtjes, P.H.J., Thunis, P., Cuvelier, K., Bedogni, K., Bessagnet, B., Honoré, C., Moussiopoulos, N., Pirovano, G., Schaap, M., Stern, R., Tarrason, L., Van Loon, M., 2007. Evaluation and intercomparison of Ozone and PM₁₀ simulations by several chemistry-transport models over 4 European cities within the City-Delta project. *Atmos. Env.* 41, 173–188.
- Vestreng, V., 2003. EMEP/MSC-W Technical report. Review and Revision. Emission Data Reported to CLRTAP. MSC-W Status Report 2003. EMEP/MSC-W Note 1/2003. ISSN 0804-2446.
- Vingarzan, R., 2004. A review of surface ozone background levels and trends. *Atmos. Env.* 38, 3431–3442.
- Weinstein, D.A., Samuelson, L.J., Arthur, M.A., 1998. Comparison of the response of red oak (*Quercus rubra*) seedlings and mature trees to ozone exposure using simulation modelling. *Environ. Pollut.* 102, 307–320.
- Werner, H., Fabian, P., 2002. Free-air fumigation of mature trees. *Environ. Sci. Pollut. Res.* 9, 117–121.
- Wesely, M.L., 1989. Parameterisation of surface resistances to gaseous dry deposition in regional-scale numerical models. *Atmos. Env.* 23, 1293–1304.
- Wilson, M., Henderson-Sellers, A., 1985. A Global archive of land cover and soils data for use in general circulation models. *J. Climatol.* 5, 119–143.
- Wittig, V.E., Ainsworth, E.A., Long, S.P., 2007. To what extent do current and projected increases in surface ozone affect photosynthesis and stomatal conductance of trees? A meta-analytic review of the last 3 decades of experiments. *Plant Cell Environ.* 30, 1150–1162.
- Zampieri, M., D'Andrea, F., Vautard, R., Ciais, P., de Noblet, N., Yiou, P., 2009. Hot European summers and the role of soil moisture in the propagation of Mediterranean drought. *J. Clim.* 22, 4747–4758.